ARTICLE IN PRESS

Acta Biomaterialia xxx (xxxx) xxx

Contents lists available at ScienceDirect

Acta Biomaterialia

journal homepage: www.elsevier.com/locate/actbio

Full length article

Batoid skin mechanical properties and morphology vary among functional swimming styles

Madeleine E. Hagood *, Joseph R.S. Alexander, Stephen Kajiura, Marianne E. Porter

Department of Biological Sciences, Florida Atlantic University, Boca Raton, FL, USA

ARTICLE INFO

Keywords:
Batoid
Mechanical properties
Tensile testing
Swimming style
Skin morphology

ABSTRACT

Batoids are cartilaginous fishes that are dorsoventrally compressed in body shape and so experience unique mechanical limitations on the effective modulation of stress forces across various swimming styles. Previous research showed that the skin of one batoid species was anisotropic, where the mechanical behavior varied between longitudinal (parallel to the vertebral column) and hoop axes (perpendicular to the vertebral column). Due to the diversity of swimming modalities employed across batoids, the patterns of mechanical behavior may vary. To explore the effect of locomotor strategy on skin mechanics, we used six species to represent styles: axial undulation (Atlantic guitarfish *Rhinobatos lentiginosus*), pectoral disc undulation (Atlantic stingray *Hypanus sabinus*, bluntnose stingray *Hypanus say*, yellow stingray *Urobatis jamaicensis*), semi-oscillation (smooth butterfly ray *Gymnura micrura*), and oscillation (cownose ray *Rhinoptera bonasus*). We tested dorsal, ventral, and composite skin samples in quasi-static uniaxial tension to failure and quantified the variability in mechanical behaviors among functional groups, regions of the body and disc, and between sexes and stress axes. We hypothesized that mechanical behaviors (tensile strain, strength, stiffness, toughness) and morphology of batoid skin would vary among swimming styles. While strain and stiffness measurements are approximate, the observed differences between groups support the conclusion that undulators had the most extensible skin whereas axial-undulators had the strongest and stiffest skin. We assessed sex differences in mechanical behaviors using Atlantic stingrays, and we found male stingrays had stronger and tougher skin than females. Lastly, we discuss the implications of dermal denticles, which may affect mechanical properties.

Statement of significance: This study provides a framework for understanding the mechanical properties of batoid skin across groups of species that utilize different swimming styles. A previous study examined just a single species, offering limited insight into the skin mechanics of a large, diverse clade of cartilaginous fishes. The results presented here include data from individual layers and composite skin samples from six species, which can be used to design mechanically specialized biomimetic and bio-inspired materials. These data provide biological ranges for batoid skin mechanics and offer insight as to the effective modulation of mechanical behavior among locomotor styles.

1. Introduction

Swimming and locomotor variability in fishes are associated with ecological niche and efficiently navigating different environments. Batoids (rays, skates, and guitarfish) are dorsoventrally flattened cartilaginous fishes, which exhibit a wide variety of swimming styles [1–3]. Batoids swim using an undulating, propulsive wave that is propelled from the mid-body out to the edges of the pectoral disc – enlarged modified pectoral fins [4,5]. In batoids, pectoral fin locomotion is generally described as either an undulatory (rajiform) or an oscillatory (mobuliform) movement, and some species modulate between those styles [6–11]. These swimming styles are classified as a continuum based on the number of propulsive waves moving across the wing during steady swimming [5,7,9,11]. Undulatory swimming is the result of small amplitude deformations, while oscillatory motion relies on large amplitude deformations of the wing [9,11]. To swim (employing either style), thrust is produced by propelling transverse waves across and through the pectoral disc. Some batoids also use the vertebral axis to produce thrust via an undulatory axial wave that moves rostral to caudal and increases in propulsive amplitude toward the tail [4,7,12]. The

* Corresponding author.
E-mail address: mhagood@tulane.edu (M.E. Hagood).

https://doi.org/10.1016/j.actbio.2025.07.070
Received 1 January 2025; Received in revised form 15 July 2025; Accepted 30 July 2025
Available online 5 August 2025

clade of batoid elasmobranchs offers a valuable and under-examined model system for researching the role of skin mechanics in locomotor variability because batoids are diverse in swimming style, body design, and skin morphology.

Many factors including body shape and ecological niche regulate the swimming capacity of different batoids. The flattened body morphology of batoids (relative to other cartilaginous fish) results in differences in the bending moments and skin structures that control the propulsive wave hydrodynamics during swimming and could impact mechanical properties of the skin. In many species of skates and rays, modification of the pectoral fins into a flattened disc has been shown to reduce drag, enhance acceleration, and improve maneuverability compared to axial-undulating and caudal-tail swimming species, like guitarfish, sawfish, and electric rays [9,13–17]. Species of guitarfishes (family Rhinobatidae) are morphologically intermediate in body shape between rays and sharks, and they swim using a combination of axial and pectoral disc undulation, generating most of the thrust in the tail [4,9]. Pectoral fin undulators tend to have flat, thin body shapes well-suited for drag reduction and maneuverability compared to oscillatory swimmers, which have thicker, more symmetrical bodies [18]. In addition to body shape, ecological habitat induces various functional mechanical limitations among batoid swimming styles [18]. For example, a kinematic study of eight species showed that benthic batoids from the genus *Hypanus* have the most undulatory fin motion, and a pelagic cownose ray *Rhinoptera bonasus* has the most oscillatory fin motion (flapping) [5,8,9,19]. Cownose rays are also comparatively more migratory and benthopelagic than other batoid species in this and previous studies [5,20]. Batoids with different swimming styles (e.g., axial-undulators such as Atlantic guitarfish *Rhinobatos lentiginosus* and pectoral undulators like yellow stingrays *Urobatis jamaicensis*) can accomplish shared behaviors, such as burying in the substrate, through different propulsive strategies [14,21]. Meanwhile, demersal species like smooth butterfly rays *Gymnura micrura* can shift the timing and duration of their swimming between undulatory and oscillatory styles depending on their location in the water column [7,9]. In theory, one of the other factors modulating locomotor efficiency among batoids is the mechanical behavior of the skin.

The functional demands on batoid skin, such as contracting a round, disc structure around a straight body axis and supporting one's body weight with the ventral skin, are met through specific arrangements of collagen fibers and scales [22]. Batoid skin is a composite of placoid scales (dermal denticles) protruding from a dermis, and internal dermal layers (the superficial stratum laxum and deep stratum compactum) arranged in alternating sheets of cross-helically oriented collagen fibers [23,24]. Dermal denticles are rooted in the stratum compactum layer of the dermis by perpendicular-running fibers, creating a reinforced collagen fiber matrix system. The collagen fiber network in the skin connects to muscles and stiffens in response to increases in internal hydrostatic pressure generated during swimming [25,26]. Collagen fiber angles in the skin of batoids range from 70 to 90° (relative to the vertebral column or longitudinal body axis) among species [23]. The denticle–collagen fiber network–muscle system connection influences the mechanical properties of the skin; subsequently differences among the collagen fiber angles and organization in various species may result in a range of skin mechanical behaviors [22]. Specifically, fiber angles near 90° (relative to the axis of applied stress) will result in greater skin extension [27], although other morphological factors also impact mechanical properties of the skin.

The variability in dermal layer organization and thickness impacts the functional mechanical behavior of batoid skin. Batoids do not have elastin in the superficial stratum laxum but rather it is found sparsely distributed in the stratum compactum, indicating the latter layer is tied to skin extensibility and mechanical properties [28]. High elastin content in the stratum compactum of West Atlantic pygmy devil ray *Mobula hypostoma* ventral skin resulted in a greater maximum breaking extension (tensile strain at max load) when stressed perpendicularly compared to ventral skin stressed longitudinally and dorsal skin along either orientation [22,28]. The pygmy devil ray has mechanically anisotropic (properties vary along different stress axes) skin, which is composed of unidirectionally organized collagen fibers that increase ventral skin thickness relative to the dorsal skin [22]. Functionally, the unidirectionally organized ventral skin of the pygmy devil ray is stronger when stressed in the direction parallel with the vertebral column, and more extensible when stressed perpendicularly to the axial plane. The thinner, orthogonally arranged (with respect to the vertebral column) dorsal skin behaves mechanically similar in both directions [22]. This diversity of morphology and mechanical behavior in the skin of one species indicates that there is likely a greater diversity among species that use different swimming styles.

The scales (dermal denticles) among species of batoids are diverse in morphology and density but not well investigated across groups. Dermal denticles of batoids are categorized by size: prickles (small), thorns (medium), and bucklers (large) [29–31]. Denticles in batoid skin are structurally composed of deep layers of dentine and superficial vitrodentine, and they are formed by minerals from dermal and epidermal cells [30,32,33]. Additionally, there is evidence that isolated denticles of thornback ray skin exhibit nanomechanical differences between denticle components: the outer vitrodentine layer has reduced stiffness but twice the hardness of the inner dentine layer [34], indicating that batoid denticles may contribute to mechanical anisotropy. Descriptions of batoid skin denticle morphology are currently limited to 11 species: 10 species of North Sea batoids [33] and the guitar ray *Pseudobatos horkelli* [31], with additional research focused on skin of the thornback ray *Raja clavata* [30]. Thornback ray denticles cover the dorsal surface of the body and tail base and exhibit diverse denticle distribution patterns and denticle morphologies among body regions and individuals [29,30,33]. In batoids, the denticle arrangements are not evenly distributed or uniform, except for the denticle cluster that appears at the base of the tail of some species [35]. The increase in denticle density at the tail base of some species may correspond to increased regional stiffness and greater collagen fiber thickness [22,27]. In sharks, dermal denticle density correlates with skin strength and toughness among juveniles [36,37]. Thus, dermal denticles among batoids may contribute to mechanical properties of the skin, like increased strength or stiffness.

Batoid skin is likely mechanically adapted to accommodate behaviors such as mating and reproduction. Species giving birth to live young, as opposed to laying eggs, must have skin compliant enough to accommodate embryonic growth before birth. Skin stretching during gestation could impact the mechanics of – and differentiate properties between – males and females of the same species. Additionally, during courtship or mating many males bite and injure their female counterparts [2,38–40]. For example, male cownose rays bite their female counterparts during courtship and mating, and mating pairs are even surrounded by other male rays that swim around and physically nudge them [39].

To reduce injuries during mating, some batoid species exhibit sexual dimorphisms in their skin. Female Atlantic stingrays *Hypanus sabinus* have greater epidermal skin thickness around the posterior pectoral fin region, where copulatory biting occurs, compared to their male counterparts [40]. Male dasyatid stingrays (*H. akajei* and *H. sabinus*) do not show increased epidermal thickness, rather their dental morphology changes seasonally to assist with gripping female stingrays during mating season [41,42]. Among urotrygonid rays, like yellow stingrays, copulatory biting is done by both sexes and in the anterior body region, rather than the posterior or wing regions [39,43]. Differences in the region of precopulatory biting among species could indicate specific adjustments to mechanical behaviors of the skin in impacted regions. Unlike other batoids, Atlantic guitarfish are not known to form distinct mating pairs or perform copulatory biting and may not experience injuries related to mating [21]. Despite this, their skin structure (dermal denticles) seems functionally more protective compared to other benthic batoids due to the large, more uniform dermal denticles that cover much of the integument.

Batoids use a variety of swimming styles, behaviors, and body morphologies to effectively modulate their swimming across ecological environments, which may impact the resulting mechanical properties of the skin. The mechanical properties of batoid skin have only been reported for one scaleless epipelagic oscillator – the pygmy devil ray [22]. We aimed to fill this knowledge gap by analyzing the mechanical behaviors among six species with varied body shapes, skin morphologies, swimming modes, and ecological niches to observe links between species ecology and skin mechanical properties. In this study, we address 1) the variability of mechanical behaviors across swimming modes, 2) the effect of sex on skin mechanics using a case species, 3) the impact of region and orientation on skin mechanics among a diverse group of batoids, and 4) the relationships between mechanics and skin morphology across a range of batoids. The six species used in this study are found in two orders, represent benthic and pelagic environments, and were functionally grouped into one of four swimming styles (axial undulation, or pectoral disc undulation, semi-oscillation, or oscillation) [6,11].

To understand the mechanical behavior of batoid skin across regions of the body and disc, we tested skin in tension along two stress axes (longitudinal, parallel to the body axis; and hoop, perpendicular to the body axis and parallel with the collagen fibers) and between skin surfaces (dorsal and ventral), to capture any mechanical anisotropy resulting from differences in fiber organization [22]. We predicted that batoid skin tested in the hoop orientation would be stronger and stiffer than skin tested longitudinally, and that skin tested along the longitudinal orientation would be more extensible, which would assist with disc undulation during swimming. To quantify regional variation in the mechanical behavior of batoid skin, we compared the mechanical properties among body regions (rostral, medial, caudal, and wing) and between proximal and distal disc regions (relative to the mid-body). Finally, we tested composite skin samples (dorsal and ventral skin connected with minimal internal tissue) to measure the mechanical properties of the entire skin structure and to compare the trends with those of dorsal and ventral skin samples.

We hypothesized that mechanical properties of the skin would vary among the specialized locomotory styles. Specifically, we hypothesized that the axial-undulators (Atlantic guitarfish) would have the stiffest and strongest skin among swimming styles, due to the combination of axial and pectoral fin undulation used in swimming. In addition, the Atlantic guitarfish body has a high surface area covered by large denticles, which may interlock. We predicted that the undulators would have the toughest and most extensible skin, whereas the oscillators would have the least strong and tough skin, and the semi-oscillators would have skin mechanically intermediate between the oscillators and undulators (as they shift between swimming styles and so must be mechanically versatile). We hypothesized that biting and reproductive biology among batoids would lead to 1) regional differences in skin mechanics across species, and 2) sex differences between male and female skin mechanical behaviors in the same species. We correlated the measured morphological and mechanical behaviors of dorsal and ventral skin and hypothesized strong relationships among variables, including increased strength and toughness associated with batoid skin from species with scales (dermal denticles, e.g., the axial-undulators and undulators). We discuss differences in these mechanical data in an ecological context – across swimming styles and habitats, and with morphological consideration.

2. Methods

2.1. Study specimens

Batoid specimens used in this study (N = 30 individuals) were functionally grouped according to swimming styles: axial-undulatory, undulatory, semi-oscillatory, and oscillatory (**Fig. S1**). Taxonomically, batoids here represent six species among five families of the orders Rhinopristiformes and Myliobatiformes. The axial undulators were represented by the Atlantic guitarfish *Rhinobatos lentiginosus* (N = 3, family Rhinobatidae). Undulators included the dasyatid rays, the Atlantic stingray *H. sabinus* (N = 12) and bluntnose stingray *H. say* (N = 2), as well as the yellow stingray *Urobatis jamaicensis* (N = 1, family Urotrygonidae). More distant myliobatiforms represented the semi-oscillatory (smooth butterfly ray *Gymnura micrura*, N = 8, family Gymnuridae) and oscillatory (cownose ray *Rhinoptera bonasus*, N = 4, family Rhinopteridae) swimming style groups (Table 1). We additionally used mechanical property data from 10 of the 12 Atlantic stingray specimens (five females, five males) to analyze variation in the mechanical properties of the skin between sexes. We used the Atlantic stingray for two reasons 1) this species represented the largest sample size in this study, including five male and female adult stingray pairs of similar sizes, since they are common to the shallow seabed of the western Atlantic coast. 2) Atlantic stingrays are sexually dimorphic in their dentition and skin thickness, making them a valuable model species for analyzing sex differences [40,42]. All species investigated are marine and estuarine water inhabitants that reside in tropical and subtropical zones (1–30 m depth) along the western Atlantic Ocean. All batoid specimens were provided by Dr. Stephen Kajiura and from mortalities at Mote Marine Laboratory, Dynasty Marine Associates, and during fishing. All data were collected pursuant to the Florida Fish and Wildlife Conservation Commission Special Activity Licenses: SAL-12–1413-SR, SAL-15–1413-SR, SAL-19–1413-SR, SAL-22–1413-SR.

2.2. Tissue preparation

All batoid specimens were stored frozen prior to dissection. Before use, each specimen was assessed for quality, and damaged or desiccated individuals were not used for sampling. There is evidence that freezing may result in the formation of ice crystals that can damage animal (human and porcine) tissues and decrease mechanical strength and stiffness [44]. Although studies examining freezing effects on the mechanical properties of fish skins are lacking, Kennedy et al. [45] reported no significant mechanical differences in the skin of frozen and fresh same-species fish, indicating that freezing may not alter the mechanical properties of fish skins. Among storage methods, it has been noted that freezing poses the least degree of structural and mechanical change to tissues [46]. Previous studies examining the mechanical properties of fish skin and spines have used frozen specimens, and the results in this study are comparable with mechanical data in the literature [36,37,45,47–49].

We thawed each specimen and dissected skin from one side of the body and pectoral disc (from the tip of the snout to the caudal edge of the pectoral disc) in a semi-circle between the internal organs and pectoral disc edge (Fig. 1; **Fig. S2**). From each individual, we dissected the lateral body that was in the best condition (e.g., fewer/no visible punctures, injuries or damage resulting from fishing or freezing). We performed skin dissections atop plastic trays to minimize damage to the skin. We cut the dissected skin into 5×5 cm^2 squares and separated the dorsal and ventral skin layers (when possible). In body regions where separation into individual skin surfaces (dorsal and ventral) was not possible, such as at the disc edge, we removed internal cartilage (when present) to the best of our ability and tested the entire composite skin sample (dorsal and ventral dermal skin layers, connective collagen fibers, and any residual mineralized structure) (**Fig. S2**). We removed as much muscle tissue as possible using a scalpel and scraper and then used a Leica EZ4W stereoscopic microscope (Leica Microsystems) to image the deep and superficial layers of the dorsal and ventral skin squares, horizontally aligned with the relative vertebral axis. Skin squares were stored in elasmobranch Ringer's solution in petri dishes and kept refrigerated no >48 h prior to imaging and mechanical testing [36,37,50]. We performed imaging prior to extracting the dog-bone pieces from the skin squares for testing.

Table 1
Descriptive information of batoid study specimens. DW = disc width, DL = disc length.

Order	Family	Species	Common name	DW (cm) range	DL (cm) range	Taxonomic authority	Swimming style	N	Sex
Rhinopristiformes	Rhinobatidae	*Rhinobatos lentiginosus*	Atlantic guitarfish	18.5–18.6	21–24.5	Garman, 1880	Axial-undulatory	3	1 M,2F
Myliobatiformes	Urotrygonidae	*Urobatis jamaicensis*	Yellow stingray	17	20	Cuvier, 1816	Undulatory	1	1F
	Dasyatidae	*Hypanus sabinus*	Atlantic stingray	12.5–27.8	12–27.2	Lesueur, 1824	Undulatory	16	6 M,6F
	Dasyatidae	*Hypanus say*	Bluntnose stingray	25.5–35	24–36	Lesueur, 1817	Undulatory	2	2F
	Gymnuridae	*Gymnura micrura*	Smooth butterfly ray	23.5–38	13–20.5	Bloch & Schneider, 1801	Semi-oscillatory	8	4 M,4F
	Rhinopteridae	*Rhinoptera bonasus*	Cownose ray	25.5–68	16.5–39	Mitchill, 1815	Oscillatory	4	1 M,3F
Total N	5	6						30	12 M,18F

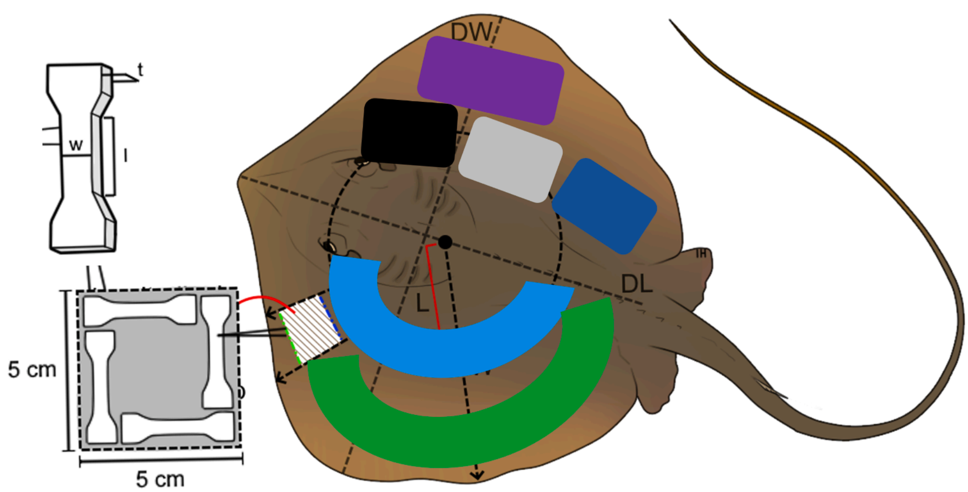

Fig. 1. Batoid dissection procedure. Atlantic stingray *Hypanus sabinus* and a cutout dissected skin square (5 × 5 cm^2) with four dog-bone shaped pieces for tensile testing (two oriented along the longitudinal axis, two along the hoop axis). Individual dog-bone cutout indicates piece dimensions: width ('w'; 5 mm), thickness ('t'; varies per piece, taken immediately prior to testing), and the region where a successful break will occur ('l', part of 10 mm total piece length). Disc width (DW, cm) and disc length (DL, cm) are labeled dotted lines on the ray body surface. Semi-circles atop the left half of the ray body denote disc regions: proximal (blue) and distal (green). Colored rectangles atop the right half of the ray body represent body region categories: rostral (black), medial (gray), caudal (navy), and wing (purple); approximately four test pieces were extracted from each body region (two per stress axis, two per disc region). Modified figure by I. Heerdegen.

2.3. Morphological analyses

To examine batoid skin morphology, we quantified the dermal denticle density (# of denticles per mm^2; when applicable) and collagen fiber angles (∡; relative to the longitudinal or axial body plane) among dorsal and ventral samples in ImageJ (NIH), using methods described in Hagood *et al.* [37]. We imaged each dorsal and ventral skin square superficially and deeply. For species with scales (dermal denticles; Atlantic stingray, bluntnose stingray, and Atlantic guitarfish, and yellow stingray) or pigmented skin (skin patches with pigmentation that resembles scales under stereoscopic microscopy; smooth butterfly ray), we calculated the denticle density as the number (count) of denticles with 60 % or more of the crown area within a 1 × 1 mm^2 box, drawn with the line tool and scaled to the 1 mm scale bar in each image (**Fig. S3**). For each skin square, we counted the number of denticles (superficially, when applicable) three times among three images, and averaged those values. Collagen fiber angles were measured using the angle tool with respect to the longitudinal, vertebral axis. Using two collagen fiber images of each skin square, we measured four total angles which were drawn with one arm parallel to an imaginary (not shown) longitudinal body axis and one arm radiating towards either the dorsal or ventral body plane (**Fig. S3**) [37]. In each skin square, the four angles were averaged to one mean angle per square. We measured the total skin thickness (mm; from the surface of the epidermis to the bottom of the deepest layer of collagen fibers) for each dog-bone piece prior to testing (below) and incorporated measurements into each tensile test to generate accurate stress-strain curves. We additionally consider thickness as a morphological variable for species-level comparisons. We used scanning electron microscopy (SEM) to observe the skin at high resolution and found variability in the density and morphology among epidermal structures compared to observations at 30x magnification.

2.4. Tensile testing

We used a hand-pressed custom tool steel die (dimensions listed in Fig. 1; Henderson Machine Inc.) to extract four dog-bone shaped testing pieces from each skin square. Two dog-bone shaped pieces were oriented along each axis of stress (longitudinal, parallel to the body axis; and hoop, perpendicular to the body axis and parallel with radiating collagen fibers; Fig. 1; **Fig. S2**). Although the piece dimensions do not conform to the ASTM standards, skin samples are non-homogenous biological material composites which by their very nature do not supply stress uniformly (**Fig. S4**).

Prior to mechanical tests, each dog-bone piece was lightly blotted with a paper towel and the thickness (mm) and width (mm) were measured with digital calipers immediately before loading to ensure accurate tensile calculations. We inserted dog-bone pieces into stainless steel metal tension clamps in an Instron E1000 Materials Testing System and tested them in quasistatic uniaxial tensile testing to failure [36,37]. Failure indicates a successful tensile test and a break along the central region of the dog-bone piece; this occurred for 87 % of tensile tests performed for this study (13 % of tests were unsuccessful and excluded prior to analyses). Tensile testing was performed with a 250 N load cell at a strain rate of 0.3 s^{-1}, using a pre-strain of 1 N to ensure samples were taut at the beginning of each test. Tensile tests are independent of one another and do not rely on the mechanical behavior of the surrounding skin or the size of the original skin sample dissected. For each tensile test, Bluehill Software (Instron, Norwood, MS, USA) uses the piece dimensions (thickness, variable; width, 5 mm; and standardized length, 10 mm) to generate a load-displacement curve standardized into a stress-strain curve. Typical stress-strain curves for each species are shown in **Fig. S4**. For each stress-strain curve, we calculated the tensile strain at maximum load (Δ length/original length, %) and mechanical properties: ultimate tensile strength (UTS, MPa), apparent Young's modulus based on engineering stress and strain measures (post-toe stiffness, MPa), and toughness (MPa). Calculations used engineering stress (not Cauchy true stress) and linear strain which should not impact measurements except at high strain when the sample deformation may alter the cross-sectional area. We did not calculate pre-toe stiffness or transition stress/strain between pre- and post-toe stiffness measurements, although future studies could incorporate these additional data.

2.5. *Statistical analyses*

Statistical analyses were performed in JMP statistical software v.16 (SAS Institute Inc., Cary, NC). We used the 30 individuals here for statistical analyses because they contributed successful mechanical test data at the same strain rate and the sample size of each group (swimming style) was three or more individuals (Table 1). In addition to the 30 individuals included in statistical analyses, we used five Atlantic stingrays to refine early mechanical testing protocols and excluded these data as specimens were tested using different parameters.

We performed non-parametric analyses, as the datasets did not meet the assumptions necessary for parametric tests (i.e. normal distribution; Shapiro-Wilk, $p < 0.05$). We used Wilcoxon Signed-Rank tests, non-parametric rank tests that compare the distribution locations of two sample populations, to detect mechanical behavior differences between the two skin surfaces, disc regions, stress axes, and sexes. To evaluate variation among functional swimming groups and body regions (variables with three or more groups), we used Kruskal-Wallis rank sum tests which rank the data from low to high and average the ranks for each group. Non-parametric analyses are based on ranking and distribution of data rather than the means (or medians). This makes non-parametric analyses more robust towards outlier points (points significantly outside the normal distribution of the dataset), which is useful when analyzing biomaterial data which are 1) highly variable, 2) not normally distributed, and 3) the true values of successful mechanical tests [22, 51–53].

We performed the described non-parametric analyses to quantify the variation among batoid skin morphology (collagen fiber angle, thickness, denticle density; $n = 345$) and mechanical behaviors (tensile strain, strength, stiffness, and toughness; $n = 345$) of dorsal and ventral skin, and the mechanical behaviors of composite skin samples. Each of the 30 batoids were represented by ~10 data points to encompass dorsal/ventral surfaces per stress axis, disc region, and region of the body. Due to the specificity of each test sample, collapsing the data further may have dampened the true range of mechanical variation. We analyzed these data between surfaces (n_1=dorsal=182; n_2=ventral=163) and disc regions (relative to mid-body, n_1=proximal=233; n_2=distal=110), using Wilcoxon tests to determine if skin morphology or mechanics varied across different body planes (Fig. 1). To examine the impact of directionality on mechanical behaviors, and observe any anisotropic behavior, we additionally analyzed the mechanical behavior data of dorsal and ventral skin samples between axes of stress (n_1=longitudinal=208; n_2=hoop=137). We assessed the variability of morphological and mechanical data from dorsal and ventral skin samples among body regions (rostral, $n = 102$; medial, $n = 154$; caudal, $n = 83$; wing, $n = 6$) and swimming styles (axial undulator, $n = 42$; undulator, $n = 107$; semi-oscillator, $n = 84$; oscillator, $n = 112$) to test our hypotheses that functional swimming groups will differ in the mechanical behavior of their skin. To quantify differences in the mechanical properties of batoid skin between sexes, we analyzed the mechanics of dorsal and ventral skin samples from five female and five male Atlantic stingrays ($n = 57$ total samples; $n = 30$ female, $n = 27$ male, approximately six test pieces from every individual) using Wilcoxon rank sum tests.

Significant results ($p < 0.05$) were further evaluated with non-parametric Dunn *post-hoc* method for all pair comparisons with joint ranking. Letters denoting significant differences among pair comparisons are included in the figures. To account for variation among differences in body size (disc width, DW) and assess the interrelatedness of mechanical and morphological measurements, we performed Spearman's correlations between tested variables and DW (cm). The correlations identified a high degree of relatedness among skin morphology, mechanical function, and body size.

We analyzed the mechanical behavior data from composite skin samples (comprising multiple dermal layers, $n = 271$), which may resemble the mechanical function of the skin as a complete system during swimming in vivo. From these analyses, we could compare trends in mechanical behaviors between composite skin samples and dorsal and ventral skin samples. We used Kruskal-Wallis tests to observe differences among the rank sums of mechanical behavior data from three swimming style groups: the undulators ($n = 132$; Atlantic stingrays, $n = 103$ and bluntnose stingrays, $n = 29$), oscillators (cownose rays, $n = 45$), and semi-oscillators (smooth butterfly rays, $n = 94$) and body regions (rostral, $n = 43$; medial, $n = 89$; caudal, $n = 73$; wing, $n = 66$). We performed Wilcoxon tests to analyze the mechanical properties of composite skin between stress axes (n_1=longitudinal=121, n_2=hoop=150) and disc regions (n_1=proximal=95, n_2=distal=176). Due to the difference in body plan, the Atlantic guitarfish samples were dorsal and ventral skin samples only, so the axial-undulators are not a functional group in the analyses of composite skin mechanical behavior.

3. Results

The results of this study represent a total of 678 individual tensile mechanical tests from 30 batoids, representing six species across five families (Table 1). These results show significant variation in skin morphology and mechanical behaviors of dorsal and ventral batoid skin among functional swimming groups, as well as differences between mechanics of skin from proximal and distal disc regions. Within a single species, we show differences in the mechanical properties of the skin between sexes. These results, as well as the strong correlative relationships among these data, suggest that morphological and mechanical properties of batoid skin are closely tied. Additionally, we found that the mechanical behaviors of composite skin samples varied among body regions and between stress axes. With each results statement, we provide the mean ± *s*.e.m. for reference, although data distributions were used for statistical analyses. For each significant result, we list the statistical test performed, the respective test statistic (H, Z, or rho), the degrees of freedom, and the p-value. P-values are provided for non-significant results.

3.1. *Skin morphology analyses*

Collagen fiber angles (relative to the longitudinal axis) varied significantly among swimming styles (Kruskal-Wallis, H(3)=81, $p < 0.0001$; Fig. 2A) and between disc regions (Wilcoxon, $Z = 2$, $p = 0.049$; Fig. 2B). Collagen fiber angles did not significantly vary among body regions ($p = 0.1$) or between skin surfaces ($p = 0.05$). However, fiber

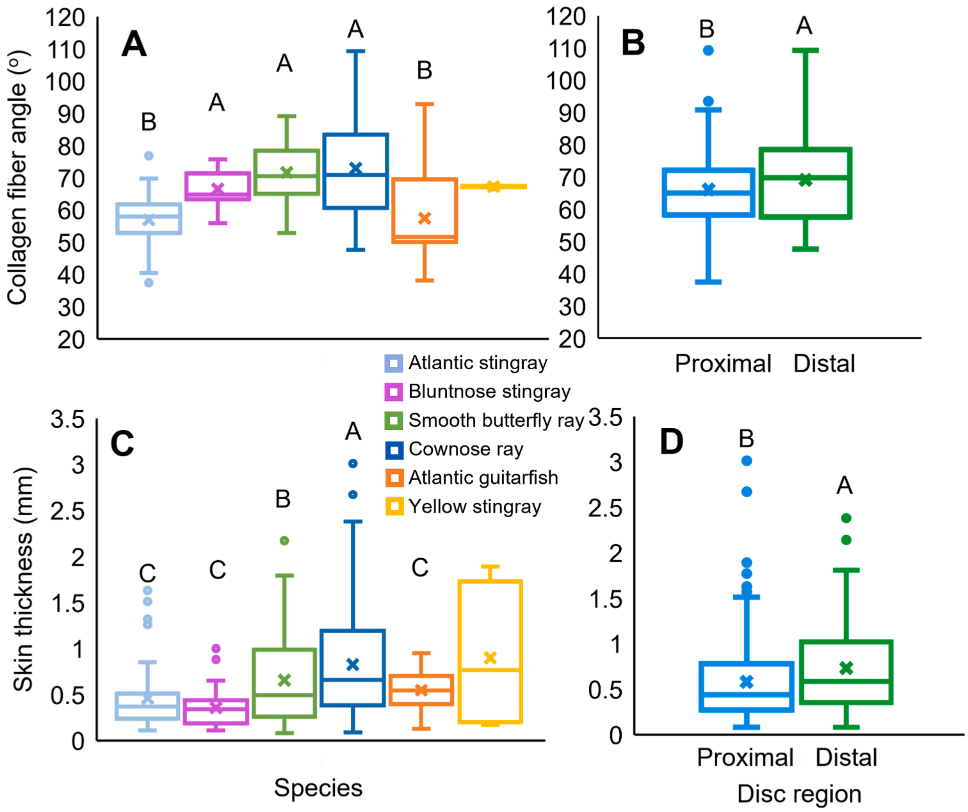

Fig. 2. Collagen fiber angle and skin thickness vary among swimming styles and between disc regions. Collagen fiber angles in batoid skin significantly varied: A) among swimming styles, the oscillatory swimmers had larger collagen fiber angles in their skin compared to the axial-undulators, semi-oscillators, and oscillators; and B) between disc regions, skin from the distal disc region contained larger fiber angles compared to skin from the proximal disc. Skin thickness varied: C) among swimming styles, the axial-undulators, semi-oscillators, and oscillators had thicker skin than the undulatory swimmers; and D) between disc regions, batoid skin from the distal disc region was thicker than skin from the proximal region. Boxes are the first and third quartiles (25 % and 75 %), the line is the median, the x is the mean, whiskers are the values to the 97.5 % quartile, and points outside the whiskers are above or below the 97.5 % quartile. Boxes with the same letter are statistically similar, per Dunn comparisons.

angles among axial-undulators were significantly ($p < 0.0001$) smaller in skin from the rostral region than the medial region (Kruskal-Wallis, H (2)=23, $p < 0.0001$). The semi-oscillators (72 ± 1°) and oscillators (73 ± 1°) had significantly larger collagen fiber angles in their skin than the undulators (61 ± 1°) and axial-undulators (57 ± 2°; Fig. 2A). Across batoids, collagen fiber angles were significantly larger in skin from the distal disc region (69 ± 1°) compared to the proximal region (66 ± 1°; Fig. 2B).

Skin thickness varied significantly among swimming styles (Kruskal-Wallis, H(3)=41, $p < 0.0001$; Fig. 2C) and between disc regions (Wilcoxon, $Z = 3.1$, $p = 0.0018$; Fig. 2D). The axial-undulators (0.5 ± 0.03 mm), semi-oscillators (0.7 ± 0.05 mm), and oscillators (0.8 ± 0.05 mm) had thicker skin than the undulatory batoids (0.4 ± 0.03 mm; $p = 0.012$, $p = 0.0048$, and $p < 0.0001$, respectively; Fig. 2C). Pooled across batoids, skin comprising the distal disc region was significantly thicker (0.7 ± 0.06 mm) than skin comprising the proximal region (0.6 ± 0.05 mm; Fig. 2D). There were no significant differences in skin thickness among body regions ($p = 0.5$) or between skin surfaces ($p = 0.2$).

3.2. Mechanical behavior analyses

The tensile strain at maximum load of dorsal and ventral batoid skin significantly varied among swimming styles (Kruskal-Wallis, H(3)=193, $p < 0.0001$; Fig. 3A) and between disc regions (Wilcoxon, Z=−5, $p < 0.0001$; Fig. 3B). The undulatory swimmers (46 ± 2 %) had significantly more extensible skin than the semi-oscillators (36 ± 2 %; $p = 0.01$), axial-undulators (15 ± 1 %; $p < 0.0001$), and oscillators (16 ± 1 %; $p < 0.0001$; Fig. 3A). The semi-oscillators had significantly more extensible skin than the axial-undulators ($p < 0.0001$) and oscillators ($p < 0.0001$). The oscillatory and axial-undulating swimmers had similarly extensible skin (Fig. 3A). Batoid skin from the proximal disc region (34 ± 1 %) was significantly more extensible than skin from the distal disc (23 ± 2 %; Fig. 3B). Tensile strain did not significantly vary between stress axes ($p = 0.07$), skin surfaces ($p = 0.2$) or among body regions ($p = 0.3$).

Ultimate tensile strength of dorsal and ventral batoid skin varied significantly among swimming styles (Kruskal-Wallis, H(3)=121, $p < 0.0001$; Fig. 3C). Batoid skin from the undulatory swimmers (16 ± 1 MPa) was significantly stronger than skin from the oscillatory (6 ± 1 MPa; $p < 0.001$) and semi-oscillatory (6 ± 1 MPa; $p < 0.0001$) swimmers (Fig. 3C). The axial-undulators (21 ± 1 MPa) had significantly stronger skin than the undulators ($p = 0.034$), oscillators ($p < 0.0001$), and semi-oscillators ($p < 0.0001$). The oscillators and semi-oscillators had similar skin strength. Dorsal and ventral skin strength did not differ between stress axes ($p = 0.3$), skin surfaces ($p = 0.1$), disc regions ($p = 0.1$), or among body regions ($p = 0.3$).

The modulus (stiffness) of dorsal and ventral batoid skin significantly varied among swimming styles (Kruskal-Wallis, H(3)=88, $p < 0.0001$; Fig. 3D). The axial-undulators (203 ± 14 MPa) had significantly stiffer skin than the undulators (112 ± 8 MPa; $p < 0.0001$), oscillators (71 ± 7 MPa; $p < 0.0001$), and semi-oscillators (67 ± 9 MPa; $p < 0.0001$) (Fig. 3D). Undulatory swimmers had significantly stiffer skin than the oscillators ($p = 0.0002$) and semi-oscillators ($p < 0.0001$), the latter two of which had similarly stiff skin. Skin stiffness did not differ between stress axes ($p = 0.5$), skin surfaces ($p = 0.3$), disc regions ($p = 0.9$), or among body regions ($p = 0.3$).

Toughness of dorsal and ventral batoid skin significantly varied

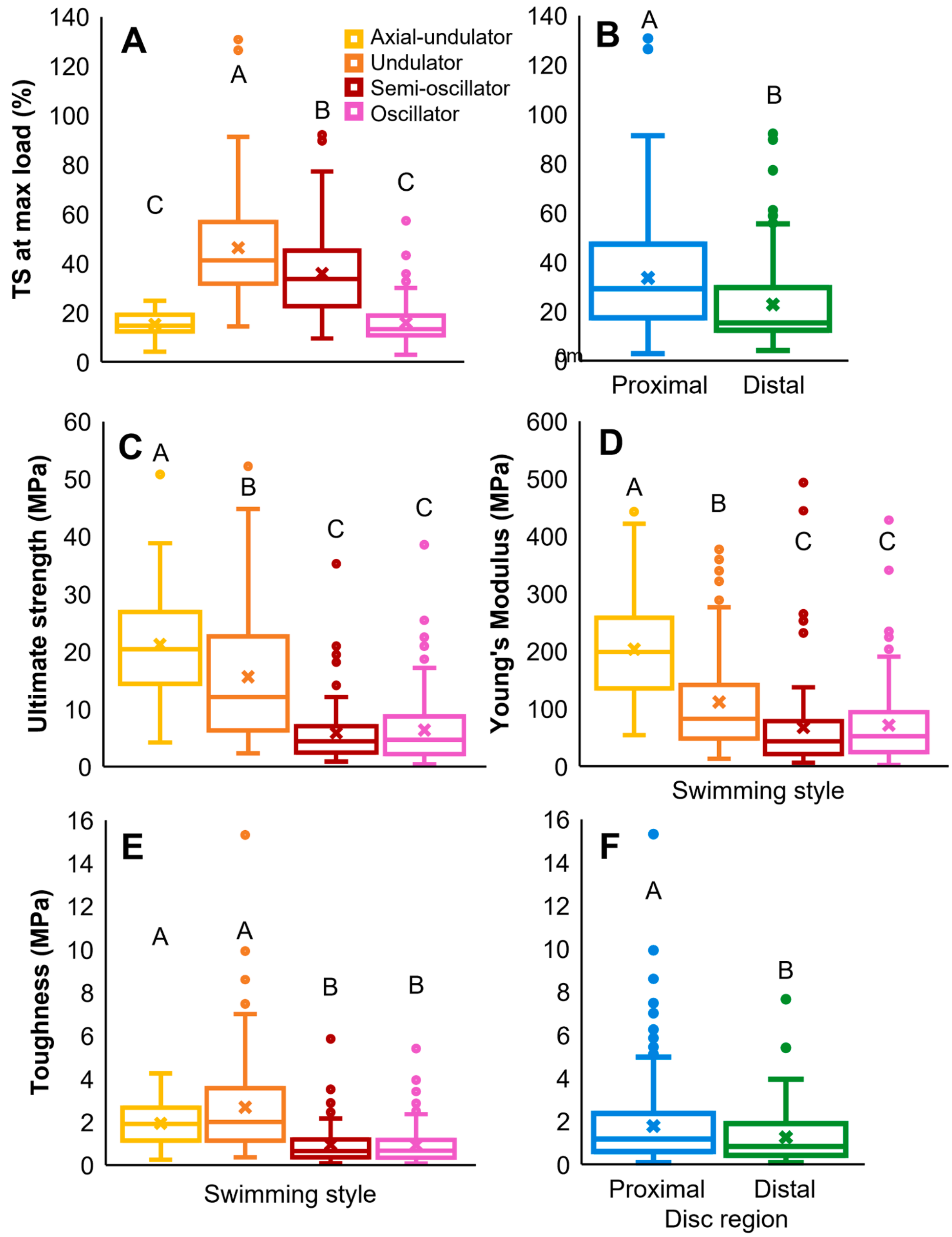

Fig. 3. Mechanical behaviors of dorsal and ventral skin samples vary among swimming styles and between disc regions. We found significant variation among batoid skin mechanics ($n = 345$, $p < 0.05$); data are combined values along both testing axes as we found no significant impact of orientation among these data. A) Tensile strain at maximum load (extensibility) varied among swimming styles, and B) between disc regions; C) skin strength varied among swimming styles; D) modulus (stiffness) varied among swimming styles; E) skin toughness varied among swimming styles, and F) between disc regions. Boxes are the first and third quartiles (25 % and 75 %), the line is the median, the x is the mean, whiskers are the values to the 97.5 % quartile, and points outside the whiskers are above the 97.5 % quartile. Boxes with the same letter are statistically similar, per Dunn comparisons. Mechanical behavior data of dorsal and ventral skin samples separated by testing axis (longitudinal and hoop) are presented in Fig. S5.

among swimming styles (Kruskal-Wallis, H(3)=111, $p < 0.0001$; Fig. 3E) and disc regions (Wilcoxon, $Z=-3$, $p = 0.004$; Fig. 3F). The undulatory (3 ± 0.2 MPa) and axial-undulatory swimmers (2 ± 0.2 MPa) had significantly tougher skin than the oscillating (1 ± 0.1 MPa; $p < 0.0001$) and semi-oscillating swimmers (1 ± 0.1 MPa; $p < 0.0001$) (Fig. 3E). The axial-undulators and undulators had similarly tough skin, as did the oscillating and semi-oscillating groups. Batoid skin from the proximal disc region (2 ± 0.1 MPa) was significantly tougher than skin from the distal region (1 ± 0.1 MPa; Fig. 3F).

As stress axis (longitudinal vs hoop) did not significantly impact any of the four mechanical behaviors analyzed above, data from dorsal and ventral batoid skin samples in Fig. 3 are combined values along both orientations. Mechanical behavior data separated by axis are shown in **Fig. S5**.

3.3. Case study: sex differences in Atlantic stingray skin mechanics

We quantified differences in the mechanical properties ($n = 57$ mechanical tests) of dorsal and ventral skin from 10 adult Atlantic stingrays (5 female, 5 male) between sexes. Stingray skin was significantly stronger (Wilcoxon, $Z = 2.5$, $p = 0.01$) and tougher (Wilcoxon, $Z = 3.3$, $p = 0.001$) for males (Fig. 4). Male Atlantic stingray skin was 40 % stronger (15 ± 2 MPa) and 33 % tougher (3 ± 1 MPa) than female stingray skin strength (9 ± 1 MPa; Fig. 4A) and toughness (2 ± 0 MPa;

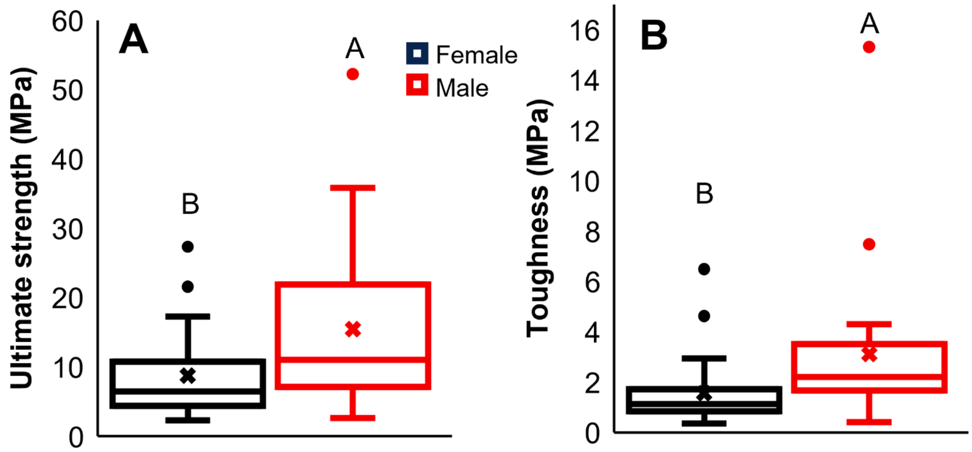

Fig. 4. Ultimate strength and toughness of Atlantic stingray skin vary between sexes. The mechanical properties of Atlantic stingray skin ($n = 57$; $N = 10$ stingrays) significantly varied between size-matched females (black, $N = 5$) and males (red, $N = 5$). A) Male Atlantic stingray skin was stronger than females ($p = 0.01$). B) Male Atlantic stingray skin was tougher than females ($p = 0.0001$). Boxes are the first and third quartiles (25 % and 75 %), the line is the median, the x is the mean, whiskers are the values to the 97.5 % quartile, and points outside the whiskers are values above the 97.5 % quartile. Letters denote statistical difference, per Dunn comparison.

Fig. 4B). Stingray skin was similarly extensible ($p = 0.1$) and stiff ($p = 0.1$) between sexes.

3.4. Spearman's correlations: morphology and mechanics

To examine the relationships between morphology and mechanical behavior, we used the dataset of dorsal and ventral skin samples from all six species to correlate the seven morphological and mechanical variables analyzed in this study, and body size (DW). Non-parametric correlations indicated significant relationships among most of the paired variables. Correlations between each pair of variables were significant, aside from one non-significant correlation between collagen fiber angle and skin thickness (Table 2). Mechanical properties – strength, stiffness, and toughness – positively correlated with each other. Denticle density and tensile strain at max load correlated positively, indicating higher denticle densities relate to greater skin extensibility among batoids. Aside from denticle density, morphological and size variables (collagen fiber angle, skin thickness, and DW) negatively correlated with the mechanical behaviors (extensibility, strength, stiffness, and toughness).

Table 2
Non-parametric Spearman's correlations of analyzed variables in dorsal and ventral batoid skin.

Variable 1	Variable 2	Spearman ρ	Prob>|ρ|
Tensile strain	DW (cm)	−0.2916	<0.0001*
Strength	DW (cm)	−0.2717	<0.0001*
Strength	Tensile strain	0.1073	0.0477*
Stiffness	DW (cm)	−0.1990	0.0002*
Stiffness	Tensile strain	−0.1589	0.0033*
Stiffness	Strength	0.9003	<0.0001*
Toughness	DW (cm)	−0.2480	<0.0001*
Toughness	Tensile strain	0.3147	<0.0001*
Toughness	Strength	0.9131	<0.0001*
Toughness	Stiffness	0.7316	<0.0001*
Thickness	DW (cm)	0.1383	0.0106*
Thickness	Tensile strain	−0.1953	0.0003*
Thickness	Strength	−0.5679	<0.0001*
Thickness	Stiffness	−0.5497	<0.0001*
Thickness	Toughness	−0.5623	<0.0001*
DenticleDen	DW (cm)	−0.3296	<0.0001*
DenticleDen	Tensile strain	0.6901	<0.0001*
DenticleDen	Strength	0.2218	<0.0001*
DenticleDen	Stiffness	0.1107	0.0411*
DenticleDen	Toughness	0.2971	<0.0001*
DenticleDen	Thickness	−0.3259	<0.0001*
CFAngle	DW (cm)	0.5040	<0.0001*
CFAngle	Tensile strain	−0.2139	<0.0001*
CFAngle	Strength	−0.2592	<0.0001*
CFAngle	Stiffness	−0.1356	0.0122*
CFAngle	Toughness	−0.2494	<0.0001*
CFAngle	Thickness	0.0584	0.2826
CFAngle	DenticleDen	−0.1143	0.0348*

[*] DW = disc width.

3.5. Composite skin mechanical behaviors

Tensile strain at max load (extensibility) of composite skin samples varied among swimming styles (Kruskal-Wallis, H(2)=47, $p < 0.0001$) and body regions (Kruskal-Wallis, H(3)=16, $p = 0.001$), and between stress axes (Wilcoxon, $Z = -4$, $p = 0.0003$) (Fig. 5). Composite samples from the undulatory swimmers (37 ± 1 %) were significantly more extensible than composite samples from the semi-oscillators (23 ± 1 %; $p < 0.0001$) and oscillators (22 ± 2 %; $p < 0.0001$), which were similarly extensible (Fig. 5A). Composite skin samples pooled across groups were significantly less extensible than composite samples from the rostral ($p = 0.002$) and caudal ($p = 0.01$) regions (Fig. 5B). Composite samples stressed along the longitudinal axis (34 ± 2 %) were significantly more extensible than along the hoop axis (26 ± 1 %; Fig. 5C).

Composite skin ultimate strength significantly varied among swimming styles (Kruskal-Wallis, H(2)=37, $p < 0.0001$) and body regions (Kruskal-Wallis, H(3)=12, $p = 0.0067$), and between stress axes (Wilcoxon, $Z = -6$, $p < 0.0001$) (Fig. 6). Composite samples from the undulatory swimmers (5 ± 0.4 MPa) were significantly stronger than samples from the semi-oscillators (3 ± 0.2 MPa; $p < 0.0001$) and oscillators (5 ± 0.9 MPa; $p = 0.01$), which were similarly strong (Fig. 6A). Pooled across groups, composite skin from the medial body region was significantly stronger than composite skin from the rostral region ($p = 0.005$; Fig. 6B). Composite skin was stronger when stressed along the hoop axis (5 ± 0.3 MPa) than stressed longitudinally (3 ± 0.3 MPa; Fig. 6C).

Composite skin stiffness significantly varied among swimming styles (Kruskal-Wallis, H(2)=8, $p = 0.02$) and body regions (Kruskal-Wallis, H (3)=23, $p < 0.0001$), and between stress axes (Wilcoxon, $Z = -5$, $p < 0.0001$) (Fig. 7). Composite samples from the undulatory swimmers (48 ± 3 MPa) were significantly stiffer than samples from the oscillators (62 ± 13 MPa; $p = 0.04$) and neither group differed from the composite sample stiffness of the semi-oscillators (41 ± 4 MPa; Fig. 7A). Altogether, composite samples were significantly stiffer from the medial and wing regions of the body than from the rostral region ($p = 0.0002$ and $p = 0.003$, respectively), and samples from the medial body region were significantly stiffer than samples from the caudal region ($p = 0.01$;

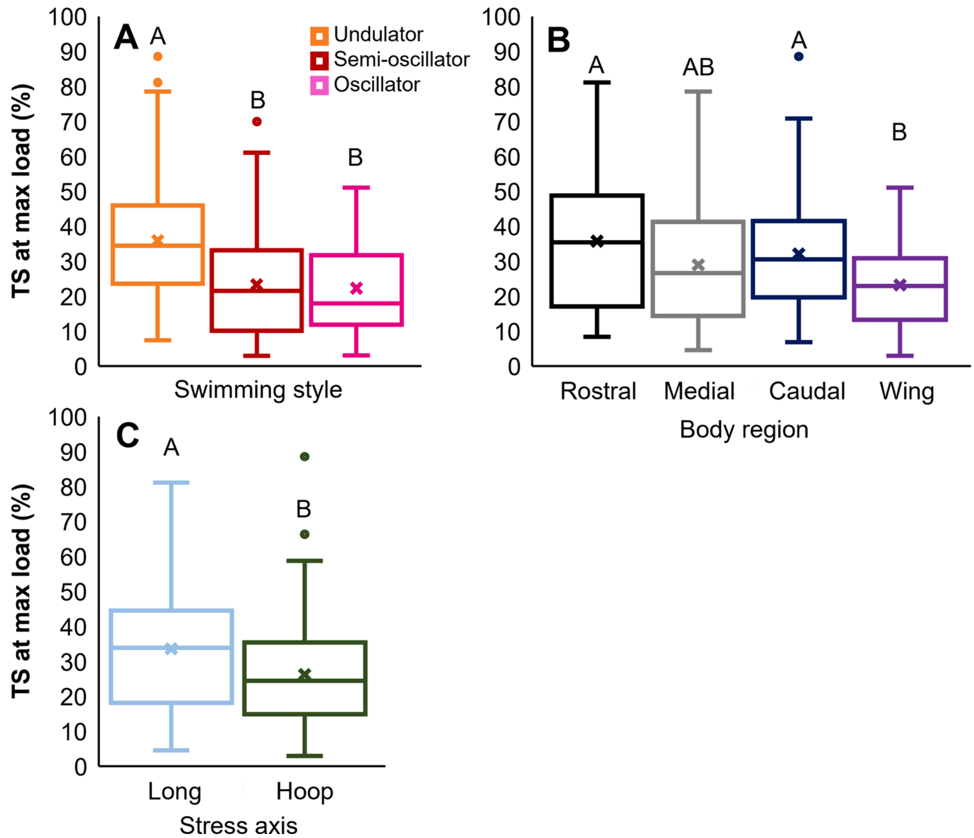

Fig. 5. Tensile strain of composite skin samples varies among swimming styles and body regions, and between stress axes. The skin extensibility of composite samples (n = 271) varied: A) among swimming styles, the undulators had more extensible skin compared to the semi-oscillators and oscillators (there were no composite samples from axial undulators); and B) among body regions, composite samples from the rostral and caudal regions were more extensible than from the wing region. C) Composite skin extensibility varied between stress axes; samples stressed along the longitudinal axis were more extensible than those stressed along the hoop axis. Boxes are the first and third quartiles (25 % and 75 %), the line is the median, the x is the mean, whiskers are the values to the 97.5 % quartile, and points outside the whiskers are values above the 97.5 % quartile. Boxes with the same letter are statistically similar, per Dunn comparisons.

Fig. 7B). Composite samples were significantly stiffer stressed along the hoop axis (59 ± 4 MPa) than stressed longitudinally (35 ± 3 MPa; Fig. 7C).

Composite skin toughness significantly varied among swimming styles (Kruskal-Wallis, H(2)=58, p < 0.0001) and between stress axes (Wilcoxon, Z=−6, p < 0.0001) (Fig. 8). Composite samples from the undulatory (0.8 ± 0.04 MPa) and oscillatory (0.8 ± 0.1 MPa) swimmers were significantly tougher than composite samples from the semi-oscillators (0.4 ± 0.02 MPa; p < 0.0001 and p < 0.0003, respectively; Fig. 8A). Pooled together, composite samples were significantly tougher when stressed along the hoop axis (0.8 ± 0.05 MPa) than stressed longitudinally (0.5 ± 0.04 MPa; Fig. 8B).

3.6. Density of epidermal skin structures

The density of epidermal skin structures significantly varied among functional swimming groups (Kruskal-Wallis, H(3)=280, p < 0.0001; Fig. 9A) and body regions (Kruskal-Wallis, H(3)=9, p = 0.03), and between disc regions (Wilcoxon, Z=−6, p < 0.0001; Fig. 9B). The undulators (153 ± 9 denticles · mm^{-2}) had significantly greater denticle density than the semi-oscillators (103 ± 2 denticles · mm^{-2}; p < 0.0001), axial-undulators (32 ± 1 denticles · mm^{-2}; p < 0.0001), and oscillators (0 denticles · mm^{-2}; p < 0.0001). The semi-oscillators had significantly greater denticle density than axial-undulators (p < 0.0001) and oscillators (p < 0.0001), and the axial-undulators had a significantly greater denticle density than oscillators (p < 0.0001). Skin from the proximal disc (92 ± 6 denticles · mm^{-2}) was significantly more denticle-dense compared to the distal disc region skin (43 ± 6 denticles · mm^{-2}). Skin surfaces did not significantly differ in denticle densities (p = 0.6). Although denticle structures were not visible in skin samples from the oscillators at 35x magnification, scales were visible using scanning electron microscopy (SEM, Fig. 10).

4. Discussion

There has been considerable investigation into the morphology and mechanical properties of elasmobranch and other fish skins published in the literature, although until now this has been limited to only one batoid species [22,28]. As batoids exhibit a wide variety of locomotory styles and body morphologies, this group of flattened fish serves as a valuable model system for examining the relationships between swimming diversity, morphology, and skin mechanics. In this study, we aimed to address the variability of mechanical behavior across batoids with different swimming styles, evaluate the impacts of sex, region, and orientation on the mechanics of dorsal, ventral, and composite skin, and explore the relationships between morphology and mechanics using skin from a variety of species. We acknowledge that strain calculations based on cross hair displacement may introduce error in absolute stiffness measurements, and therefore, the mechanical findings should be interpreted primarily in a comparative context rather than in absolute terms. While the absolute measures may vary from the reported values, the comparative trends remain consistent and interpretable. We found significant differences among the four swimming modalities in skin morphology and mechanics, including strength, stiffness, toughness, skin thickness, and denticle density. Composite batoid skin varies among body regions (rostral medial, caudal, and wing) and between stress axes;

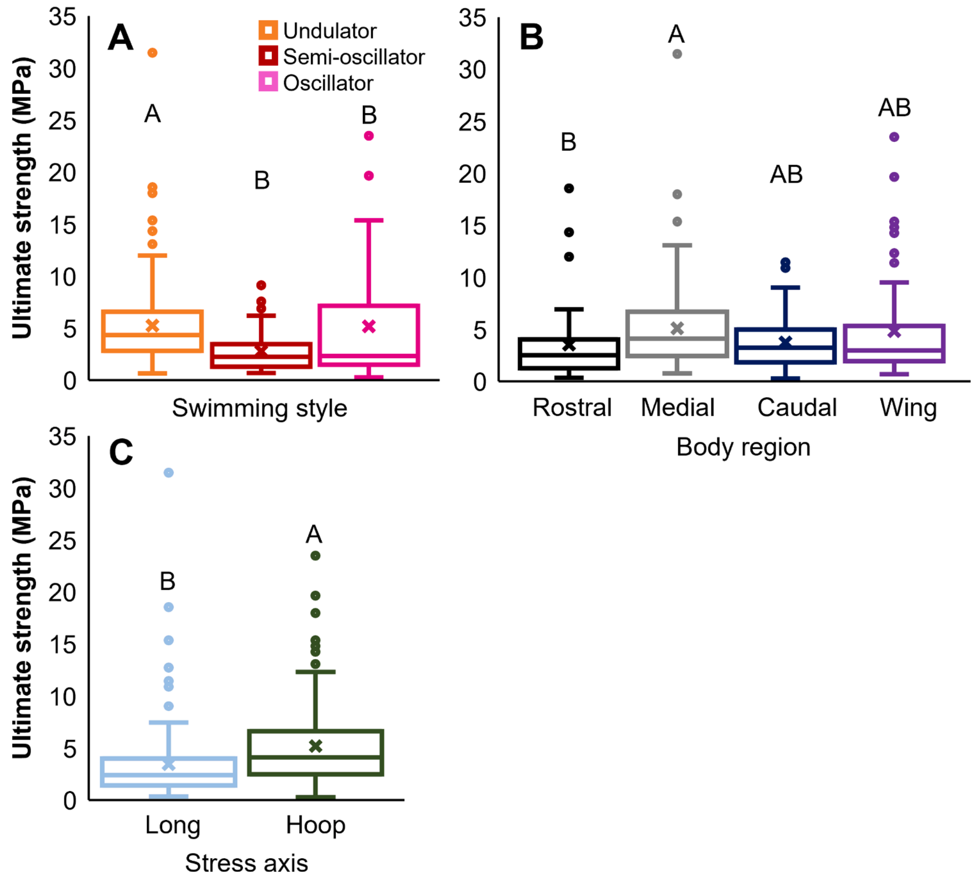

Fig. 6. Ultimate strength of composite skin samples varies among swimming styles and body regions, and between stress axes. Composite skin strength (n = 271) varied: A) among swimming styles, the undulators had stronger skin than the semi-oscillators and oscillators; and B) among body regions, composite skin was stronger from the medial region than the rostral region. C) Composite skin was stronger stressed along the hoop axis than stressed longitudinally. Boxes are the first and third quartiles (25 % and 75 %), the line is the median, the x is the mean, whiskers are the values to the 97.5 % quartile, and points outside the whiskers are values above the 97.5 % quartile. Boxes with the same letter are statistically similar, per Dunn comparisons.

samples were mechanically anisotropic, behaving stronger, stiffer, and tougher when stressed along the hoop axis (perpendicular to the vertebral axis, with the orientation of collagen fibers) and more extensible stressed longitudinally (parallel to the vertebral axis, opposing the orientation of collagen fibers). When discussing composite skin samples, we provide the median as it is a better representation of the data (less impacted by outliers) to accompany statements of the results (although distributions were used for analyses). This study supplies ecological and functional context to understanding the relationship between batoid skin mechanical properties and swimming. To the authors' knowledge, the case study using Atlantic stingrays is the first evidence of sex differences in the mechanical properties of batoid skin. Additionally, these results provide literary reference for mechanical property data of a diversity of batoid species and may reveal potential underlying links among species or swimming modes that could assist with classifying batoids taxonomically and ecologically.

4.1. Skin morphology (collagen fiber angle and skin thickness) varies across batoids

Skin morphology, collagen fiber angle and thickness, varies among swimming styles and disc regions and may alter mechanical behavior. The collagen fiber angles (relative to the vertebral axis) among batoids here ranged from 40 to 110°. Fiber angles in skin from the distal disc region were larger on average and had a wider range (~69°, 60–80°) compared to skin from the proximal region (~66°, 60–70°; Fig. 2B). Skin from the semi-oscillators and oscillators contained collagen fiber angles that were 10–15° larger than the average angles among axial-undulators and undulators (Fig. 2A). Oscillatory swimmers generate thrust in lift-based propulsion around the pectoral disc, so larger fiber angles may provide greater extensibility in this region [54–56]. Our morphological results support previous research showing that swimming style and body shape are linked among batoid groups. For example, body morphology and wing aspect ratio correspond to shifts between undulatory and oscillatory swimming [9,11,18,57]. Therefore, collagen fiber angles, which are based on body morphology and location relative to the vertebral axis, are a naturally variable feature of the skin among batoids with diverse body shapes. Regional variation in collagen fiber angles was observed in pygmy devil ray skin, in which fiber angles vary from 45° near the vertebrae to smaller angles (25–30°) in the pectoral body region [28]. Similarly, collagen fiber angles in shark skin also depend highly on the anteroposterior body location and have been reported from 0° (at the caudal fin) to 90° (in the occipital region), although most longitudinal angles are between 40 and 60° [23,25,27]. The ranges of fiber angles we report may differ from that of pygmy devil ray skin [28] as we performed sampling across more distant regions (from the rostrum to the pelvic fin and the vertebral axis to the wing tip) and more diverse species.

Consistent with previous research, we found skin thickness varied among swimming styles and between disc regions. The undulators had the thinnest skin among swimming groups (Fig. 2C), which may reflect known differences in body morphology and assist in maneuverability [11,18]. Across swimming groups, batoid skin from the distal disc region was ~0.15 mm thicker than skin from the proximal region (Fig. 2D). These results suggest that thicker skin towards the disc edges, farther from the midline, may produce an adequate lift around the pectoral disc,

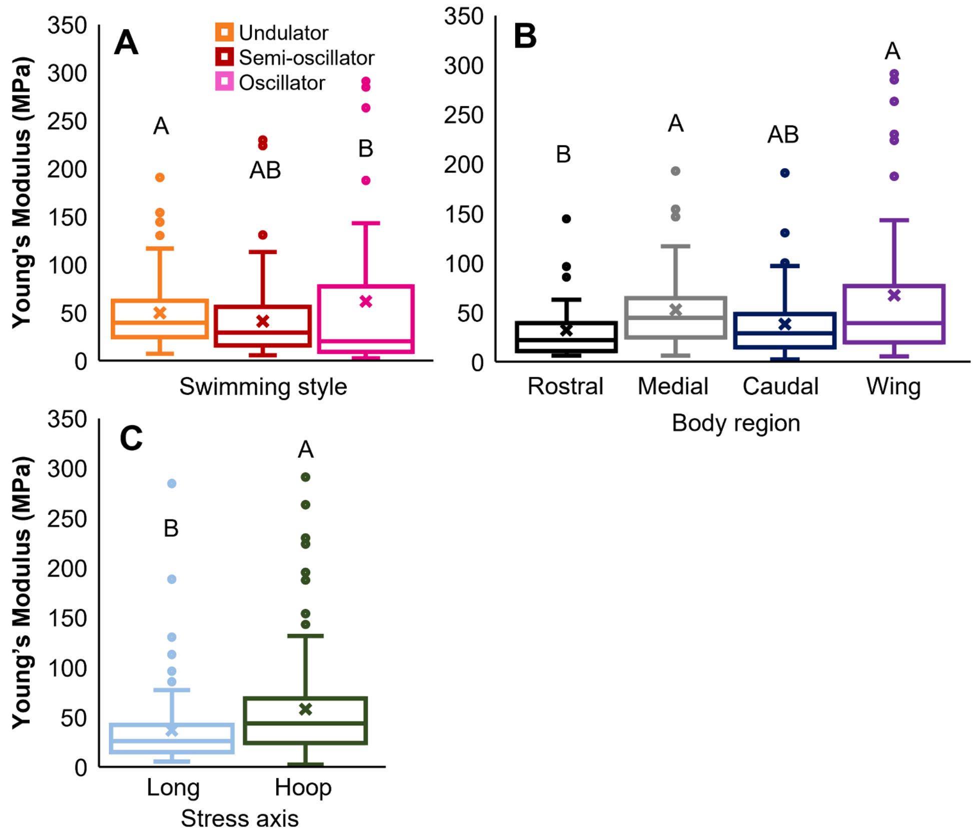

Fig. 7. Modulus (stiffness) of composite skin samples varies among swimming styles and body regions, and between stress axes. The stiffness of composite skin ($n = 271$) varied: A) among swimming styles, the undulators had stiffer skin than the oscillators, and the semi-oscillators were intermediate; B) among body regions, composite samples were stiffer from the wing and medial regions than from the rostral region, and the caudal region samples had intermediate stiffness; and C) between stress axes, composite skin was stiffer when stressed along the hoop axis than longitudinally. Boxes are the first and third quartiles (25 % and 75 %), the line is the median, the x is the mean, whiskers are the values to the 97.5 % quartile, and points outside the whiskers are values above the 97.5 % quartile. Boxes with the same letter are statistically similar, per Dunn comparisons.

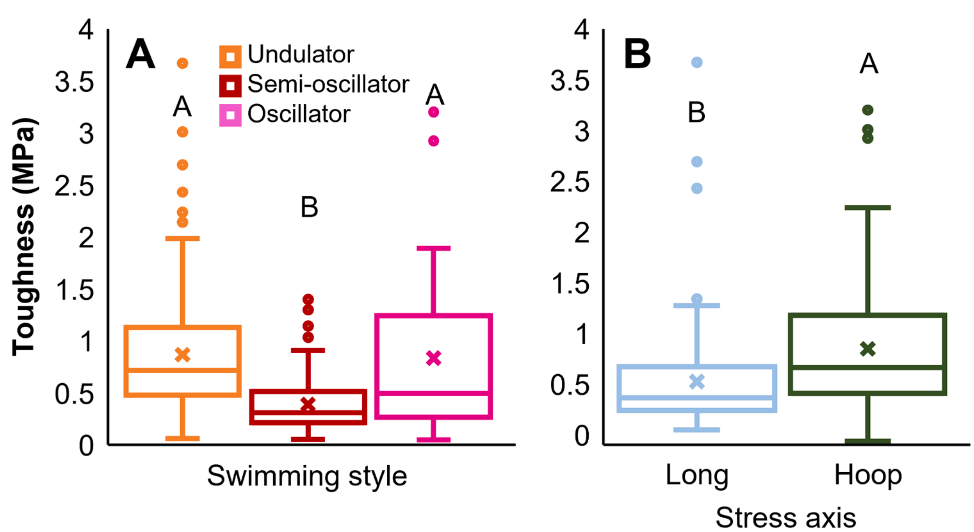

Fig. 8. Toughness of composite skin samples varies among swimming styles and between stress axes. The toughness of composite samples ($n = 271$) varied: A) among swimming styles, the undulators and oscillators had tougher composite skin than the semi-oscillators; and B) between stress axes. composite samples stressed along the hoop axis were tougher than those stressed longitudinally. Boxes are the first and third quartiles (25 % and 75 %), the line is the median, the x is the mean, whiskers are the values to the 97.5 % quartile, and points outside the whiskers are values above the 97.5 % quartile. Boxes with the same letter are statistically similar, per Dunn comparisons.

particularly among the oscillators [4,7,11].

Early research on the mechanical behavior of batoid skin used one species with an unreported sample size of total individuals [22]. Hypotheses posed in this study are therefore based on interpretations of data collected from small or unknown sample sizes. Practically, sample sizes of fresh biological materials for mechanical testing vary across the

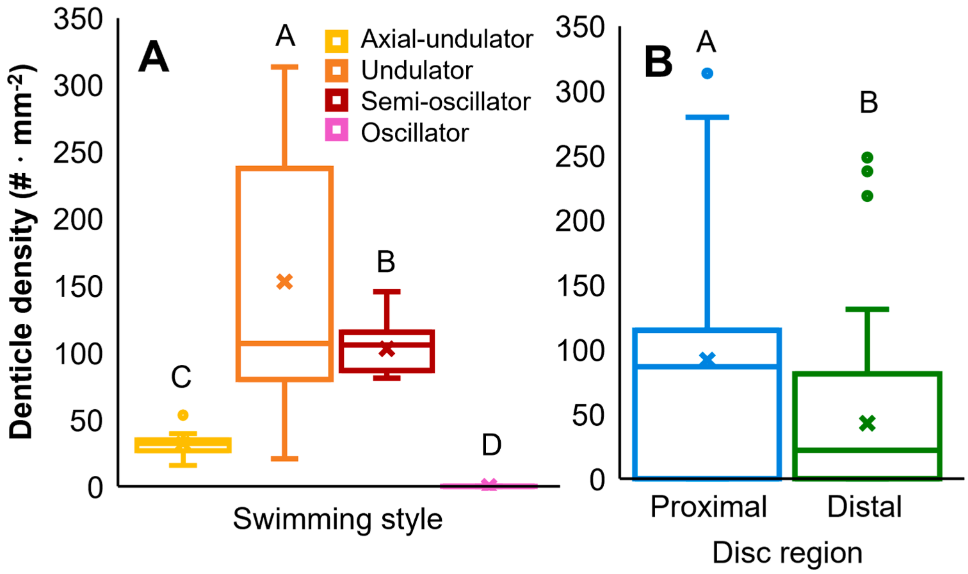

Fig. 9. Density of epidermal skin structures (dermal denticles) varies among swimming styles and between disc regions. A) The undulators had the greatest density of denticles, followed by the semi-oscillators, the axial-undulators, and the oscillators had the least (0 denticles). B) Denticle density was greater in skin from the proximal disc region compared to the distal disc. Boxes are the first and third quartiles (25 % and 75 %), the line is the median, the x is the mean, whiskers are the values to the 97.5 % quartile, and points outside the whiskers are values above the 97.5 % quartile. Boxes with the same letter are statistically similar, per Dunn comparisons.

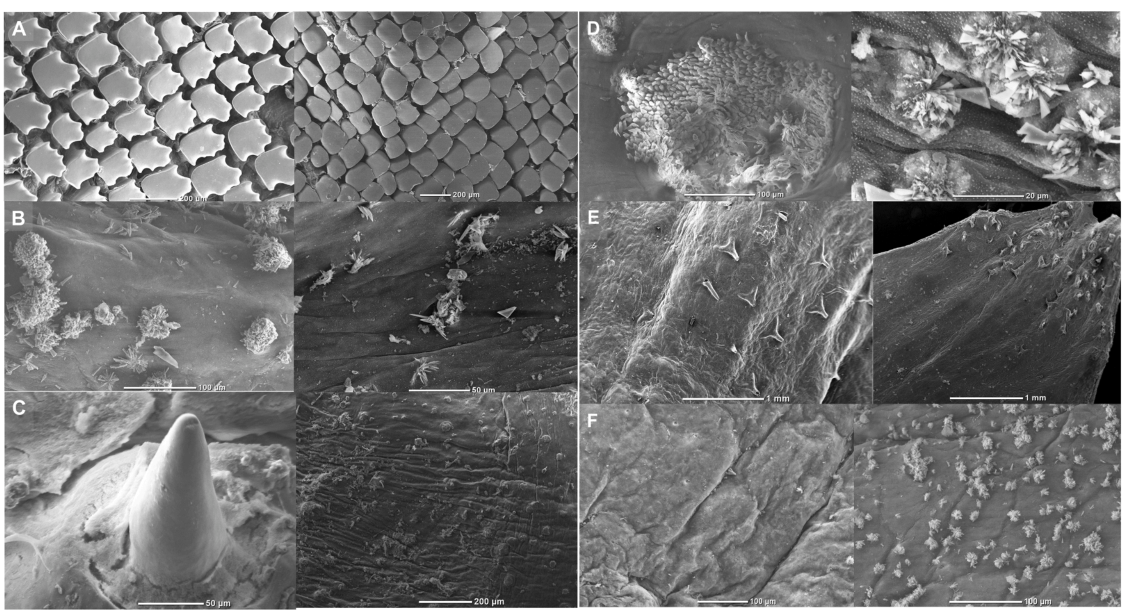

Fig. 10. Skin structures among batoid species and body regions. A) Atlantic guitarfish skin from the rostral (left) and caudal (right) body regions. B) Atlantic stingray skin from the rostral (left) and medial (right) regions. C) Bluntnose stingray skin from the rostral (left) and wing (right) regions. D) Smooth butterfly ray skin from the rostral (left) and wing (right) regions. E) Cownose ray skin from the rostral (left) and caudal (right) regions. F) Yellow stingray skin from the rostral (left) and caudal (right) regions. Images were taken with scanning electron microscopy (SEM) at variable magnifications to present the broad range of denticle structure morphology and density observed. Images chosen for this figure were limited to dorsal batoid skin to highlight differences in skin morphology in a single region.

literature. Sample sizes of shark skin data sets range from one or two individuals [25,27] to samples with mixed sizes of two, three, and four individuals per species [36]. Mechanical testing of fresh teleost skins has been reported in sample sizes of four and five fish per species [58] to groups of three, five, and eight fish per species [45].

In this study, we may have been able to reduce the chances of type II errors by increasing the sample size (which would increase power) but due to the limited and opportunistic nature of specimen collection, this was not feasible. When sample sizes are small and power is low, effect sizes must be large to detect statistical significance [59]. Thus, it is not likely that statistically significant differences reported here are errors due to small sample sizes.

4.2. *Does functional swimming style impact mechanical behavior?*

We hypothesized greater skin extensibility and toughness among undulatory swimmers and stiffer, stronger skin among the axial-undulators based on previous research examining forces and pressure gradients along the bodies of batoids employing different swimming styles [4,5,9,11,18,54,60]. The mechanical behavior of dorsal and ventral samples of batoid skin varied among the functional swimming styles, wherein the undulators had the greatest range of percent extension and the most extensible skin (14–130 %), followed by the semi-oscillators (9.5–92 %), whose average skin extension was still twice that of the oscillators and axial-undulators (Fig. 3A). Similar skin extensibility among undulatory and semi-oscillatory swimmers may imply a functional need for mechanical extension underlying the undulatory motion of demersal species [9,19]. Undulatory swimmers have reduced (catenated) calcification of their skeleton [11]. In addition to reduced calcification, many dasyatid rays also have joint staggering between radials of the distal wing. This pattern creates a lighter, more flexible, skeleton with additional spacing between joints, which could lead to fewer connections with the skin and thus higher skin extensibility compared to semi-oscillators and oscillators [11]. Meanwhile, axial-undulating and oscillating swimmers have greater calcification of the skeleton, which impacts wing stiffness and may explain the reduced skin extensibility we observed among these groups [11]. Skin extensibility may therefore be dependent upon the internal structurization of species, although batoid skin seemed to fall within a similar range of extensibility across species. Batoid skin extensibility (tensile strain) here ranged from 3 to 130 %, which is similar to the range published for pygmy devil ray skin (30–120 %) [22]. As collagen fibers have been noted as extending up to 10–20 % prior to breaking [12,23], the ability of batoid skin to extend up to 6x the purported extensibility is considerable.

We found that axial-undulators, like Atlantic guitarfish, had the strongest skin among swimming styles (4–50 MPa; Fig. 3C). Batoid skin strength spanned over two orders of magnitude (0.4–52 MPa), with groups of axial-undulators and undulators having skin stronger than 50 MPa. These results indicate that axial-undulators may need stronger skin to provide more efficient energy transfer during swimming, potentially as a response to their calcified axial skeleton and use of the tail in generating thrust [9]. Pectoral fin undulators have a less-calcified skeleton than axial-undulators [11], so it is interesting that the two groups of undulating batoids here both had skin 2–3x stronger than the semi-oscillators and oscillators regardless of the degree of internal calcification. Compared to previous studies, we found axial-undulators (~21 MPa) and undulators (15.6 MPa) had strength comparable to the strongest pygmy devil ray skin (~18 MPa), whereas semi-oscillators (5.8 MPa) and oscillators (6.3 MPa) had skin strength resembling the low end of the range seen in pygmy devil ray skin (2–3 MPa) [22]. Oscillators like the cownose ray have a high thickness ratio and symmetrical wings that enhance necessary lift-based thrust production and minimize drag during high-speed, steady cruising in pelagic environments [18,56,60]. Thus, oscillatory motion may benefit from reduced skin strength and stiffness that would minimally resist deformation and stress forces and could allow for easier movement given the high mineralization of the skeleton [11].

We recorded batoid skin stiffness ranging between 2.3–492 MPa and found that the axial-undulators had the stiffest skin, averaging approximately 200 MPa, among functional swimming styes. Undulatory motion affects swimming speed and flexibility through the degree of flexural or bending stiffness [11,61]. We found axial-undulators had 2x as stiff skin as the undulators, and 4x as stiff as the semi-oscillators and oscillators (Fig. 3D), suggesting these batoids use their skin to efficiently transmit greater force down the body and possibly that they experience higher internal hydrostatic pressure changes due to use of their axial skeleton to swim. Here, most batoid skin stiffness measured between 30 and 300 MPa, which is greater than the stiffness reported for bony fish skin (6–20 MPa) and tendon (1.2–1.4 MPa) [62–64]. We found skin stiffness also reached the lower range of batoid propterygia stiffness (140–2533 MPa) [65] and was comparable to (and sometimes stiffer than) juvenile shark skin (14–276 MPa) [37]. These results suggest that the mechanical range of skin stiffness may be similar across elasmobranch fishes despite differences in morphology and locomotory style. It is necessary to acknowledge that using cross hair displacement can provide inaccurate quantitative skin stiffness measures, but the information reported is still qualitatively meaningful.

We found that batoid skin toughness ranged from 0.1 to 15 MPa, and that the undulating batoids (axial-undulators and pectoral undulators) had skin 2–3x as tough as the semi-oscillators and oscillators (Fig. 3E). The semi-oscillators had skin of similar strength, stiffness, and toughness as the oscillators. These results indicate that semi-oscillators have similar skin mechanical functionality to oscillators and are not mechanical intermediates between undulators and oscillators (as hypothesized). Additionally, these data suggest that species of semi-oscillators and oscillators may be less reliant on the mechanical behavior of the skin for effective force transmission during swimming, and more reliant on the wing shape and mineralized skeletal elements [11,18]. These groups potentially meet the functional demands of swimming through their internal calcification and body morphology [11,18]. Our reported toughness range cannot be directly compared with other batoids because the toughness of pygmy devil ray skin was not described by Rajaram and Ramanathan [22]. However, we found batoid skin toughness within the range of skin toughness from coastal shark species (2.5–16 MPa) and from juvenile sharks (0.5–40 MPa) [36,37]. In all, batoid skin mechanical properties were comparable with other marine biological materials, such as batoid propterygia and skin from other elasmobranchs (e.g., sharks and the pygmy devil ray) [22,36,65]. It is worth noting that the axial-undulating batoids represent the functional group with skin mechanical behavior most resemblant of sharks, fellow axial-undulators.

Composite skin samples, which consisted of connected dorsal and ventral skin but had skeletal elements removed, exhibited similar mechanical variation among swimming style groups as in dorsal and ventral skin samples (Figs. 5–8). Composite skin mechanical behavior may be more like the mechanics of the entire skin structure, and results could be a better representation of skin mechanics during in vivo swimming. We analyzed the mechanical behaviors of composite skin among three functional swimming styles: undulators, semi-oscillators, and oscillators (there was no axial-undulator group of composite skin data due to differences in body and skin morphology). Composite skin from the undulators was 1.5x as extensible (35 %, median), and nearly 2x as strong (4 MPa, median), as median values of composite skin from the semi-oscillators (21.5 % and 2.2 MPa) and oscillators (17.9 % and 2.3 MPa; Figs. 5A and 6A). The median composite skin stiffness among the undulators (37.8 MPa) was nearly 2x that of the oscillators (20 MPa), and the semi-oscillators were intermediate (29 MPa; Fig. 7A). Interestingly, the semi-oscillators had similar composite skin stiffness as both other functional groups and had the least tough composite skin. Composite skin from the undulators (0.6 MPa) and oscillators (0.5 MPa) were 50 % and 33 % tougher, respectively, than skin from semi-oscillators (0.3 MPa; Fig. 8A). This result is unlike the dorsal and ventral skin mechanics of the semi- and oscillating swimmers, wherein the groups had similarly tough skin, distinctly weaker than the undulators. Differences between the mechanical toughness of composite skin compared to dorsal and ventral skin suggest that oscillating species achieve toughness through the multilayered composite skin structure, which may be tougher with the additional mineralized layers intact [11]. Additionally, recent evidence shows that the proportion of muscle fiber types varies between undulatory and oscillatory batoids, with undulators having a higher percentage of fast-white, glycolytic muscle fiber compared to the oscillatory batoids which have more slow-red, oxidative fibers [66]. Variation of muscle fiber types may provide a mechanism behind some of the trends among composite skin samples' mechanical behaviors we observed. For example, red muscle fibers among oscillators facilitate steady migratory and cruising behavior, whereas white muscle fibers among undulators assist with rapid responses such as prey capture, predator avoidance, and burying behaviors [66–69]. The higher content of red fibers in the oscillators might contribute to whole body toughness, while the higher proportion of white fibers in the undulators could require greater extensibility and stiffness of composite skin to quickly transmit high forces during rapid response behaviors.

4.3. Does batoid skin mechanical behavior vary across regions of the body or disc?

The mechanical properties of batoid skin were analyzed among body (rostral, medial, caudal, and wing), and between disc (proximal and distal), regions. Due to the mechanical limitations placed on different areas of batoids' bodies, we hypothesized that regions of the body near the center (medial region; proximal disc) would have stronger and stiffer skin, and regions further from the body (rostral, caudal, wing; distal disc) would have more extensible skin. Although results from dorsal and ventral skin samples indicate that disc regions differ mechanically, the resulting trends differed from what we predicted. Across batoids, the proximal disc skin was nearly twice as extensible (28.8 %, median) and 50 % tougher (1.2 MPa, median) than skin from the distal region (15.3 % and 0.8 MPa; Fig. 3B and F). Mechanical properties of skin from the proximal disc correlated with the skin morphology (smaller fiber angles and thinner skin) in this region (Fig. 2; Table 2). Additional mineralized structures may contribute to flexural and wing stiffness and subsequently, skin near the vertebral axis would benefit from increased toughness, potentially serving as protective [11]. The mechanical behavior of dorsal and ventral skin did not vary among body regions. Due to differences in the mechanical requirements of batoids across swimming styles, it is possible that species specific trends in regional mechanics were not detectable across pooled data. However, within swimming styles, axial-undulators were the only group to show regional differences in collagen fiber angles, which were smaller in skin from the rostral region relative to the medial region. This specific difference is likely related to the use of the rostrum in digging and burrowing behaviors of axial-undulating batoids [9].

Unlike dorsal and ventral skin samples, the mechanics of composite skin samples varied among body regions. Composite skin from the rostral and caudal body regions was 5–10 % more extensible than from the wing region (Fig. 5B). This extensibility may be related to the reduced integration of skeletal structures in these areas and could assist in minimizing injury in the caudal region during mating [11,40]. The rostral region is also the site of prey excavation, propulsive wave origination and propagation for swimming, which would functionally benefit from greater extensibility to initiate undulatory movement [8,9,19]. Composite skin from the medial region was 2x stronger than skin from the rostral region (Fig. 6B). Likewise, skin from the medial and wing regions was 1.5–2x stiffer than skin from the rostral region (Fig. 7B), suggesting greater resistance to deformation in the medial and wing regions of the body. These results fit with the current understanding of stress placed on the skeletons of batoids and variability in the requirements for flexural stiffness among swimming modes. Additional joint-staggering among undulatory batoids and cross-bracing among oscillatory batoids are found in the medial and distal portions of the wings and would increase strength and stiffness in these regions [11]. Undulatory species experience increased bending stresses near the wing edges, whereas oscillatory species rely on critical cross-bracing at load-bearing medial regions of the wing [11] and are most flexible at the wing tip [4,5,9,60]. During oscillatory locomotion, the radials are flexed dorsally by dorsal adductor muscles and ventrally by smaller ventral abductors, and the wingtips of rapid oscillators touch behind the dorsal body surface indicating the need for stiffness (to transmit muscle force) in the wings [9,11].

4.4. Mechanical differences between stress axes and skin surfaces may be species-specific

Based on previous research of mechanical properties in the skin of other batoid and fish species, we theorized mechanical anisotropy among batoid skin [22,25,27,28,37,45]. These data do not indicate an impact of testing orientation (longitudinal or hoop) on mechanics of dorsal or ventral skin when pooled across batoids, even when data are separated between skin surfaces. Observable differences in stress axis application may not appear for the mechanical properties of some batoid species' skin due to the near 90° angles formed by the collagen fiber network (resulting in the same degree of straightening to meet each stress axis) [12,23]. It is additionally possible that type II errors in these data falsely indicate a lack of significant differences, and differences may be found given a larger sample size [59].

Results of this study do not support our hypothesis that mechanical behavior across batoids would differ between dorsal and ventral skin surfaces. Undulating swimmers may benefit from equal dorsal and ventral skin mechanics to support undulatory movement and maneuver in their benthic environments and may not require a uniform collagen fiber arrangement in their ventral skin. It is possible that cross-bracing in the skin of oscillating species like the pygmy devil ray may add weight to the body and additional loading stress to the ventral skin [11,22,28]. For this reason, anisotropy in batoid skin mechanics may be a characteristic limited to the pygmy devil ray, or to oscillators (here one species), and therefore could be too small of an effect to detect in this dataset.

Although dorsal and ventral skin samples did not exhibit mechanical anisotropy, composite skin did. Across batoids, composite skin samples were 50 % more extensible stressed along the longitudinal (vertebral) axis, and 1.5x stiffer, 1.5x stronger, and 2x tougher stressed along the hoop axis (Figs. 5C, 6C, 7C, and 8B). These results contrast with the published anisotropy in pygmy devil ray skin, which extends farther along the hoop axis and is stronger and stiffer stressed longitudinally, although composite skin may not be comparable with devil ray ventral skin [22]. Anisotropic behavior also depends on the arrangement of structures in the skin (collagen fibers and denticles), which varies among batoids, making this behavior potentially specific to the species or swimming style used [18,33]. The anisotropic results here are like the trends reported for the mechanical behavior of shark skin, which highlights the similar mechanical limitations placed on elasmobranchs by their fluid environment [25,27,37]. The mechanical properties of composite batoid skin may therefore correspond to swimming demands placed on the entire body across functional swimming styles.

4.5. Do the mechanical properties of Atlantic stingray skin vary between sexes?

Results from this study provide evidence of sex differences in the mechanical properties of batoid skin using a single species with known sexual dimorphisms as a case study. Female Atlantic stingrays have greater dermal thickness relative to males, and this is proposed to provide protection to females during copulation [40]. Due to the negative relationship between mechanical behaviors and skin thickness observed in shark skin between sexes [37], we hypothesized that the thicker skin of female stingrays would result in weaker (less strong and tough) skin. Results of the case study support this, indicating male Atlantic stingrays have stronger and tougher skin, although skin thickness did not differ between sexes here. Male stingray skin was 50 % stronger and 50 % tougher than skin from size-matched female stingrays, indicating that male stingray skin may be mechanically advantageous and capable of withstanding higher stress forces (Fig. 4). In preparation for mating, the morphology of male stingray dentition changes seasonally from a female-like molariform shape during non-mating seasons to a sharp, cuspidate shape [42]. Bite wounds observed on male stingrays are theorized to occur as a result of chance premating encounters among males, as it is not likely that they are able to visually discriminate females [40]. Additionally, the sharp tooth morphology of male stingrays during mating season results in precopulatory bites that would be stimulatory to a female but may sever tissue from the thinner dermis of a male [40]. The greater dermal thickness reported for female stingrays may be related to increased adipose tissue or less compacted fibers that result in an insulative buffer that minimizes internal injuries, but is easier to fracture than male stingray skin [40]. We posit that stronger and tougher skin among male stingrays may reduce injury or tearing of the thinner dermis during precopulatory encounters with other males. These data support the functional mechanism that thicker skin may produce weaker skin mechanics (strength and toughness), as has been published for skin from Gulf hagfish *Eptatretus springeri* and juvenile female sharks [37,45].

4.6. Relationships between morphology and mechanics of dorsal and ventral skin

The morphology (collagen fiber angle, skin thickness, dermal denticle density) and mechanical behaviors (tensile strain, strength, stiffness, toughness) of dorsal and ventral batoid skin samples were highly intercorrelated with each other, as well as with individual body size (DW) across all 30 batoids. Skin strength, stiffness, and toughness were strongly positively correlated with each other (Table 2). Stiffness and tensile strain were the only two negatively related behaviors, highlighting this trade-off in mechanical function. This inverse relationship is a well-known result of collagen fiber orientation among mechanically anisotropic fish skins [22,25,27,37,45,64]. Mechanical properties (strength, stiffness, and toughness) positively correlate with body size (DW), suggesting that a larger body may relate to stronger, stiffer, and tougher skin. A large body could pose challenges to maneuverability and rapid response initiation and may require stronger and stiffer skin to power thrust and efficiently modulate muscle force, particularly since rays are negatively buoyant like other cartilaginous fish [14]. Disc width positively correlated with skin thickness and with collagen fiber angle, supporting the morphological results detailed above. As skin thickness increased, strength, stiffness, and toughness decreased (Table 2). The negative relationships between mechanical behaviors and skin thickness indicate that thicker skin is not necessarily mechanically advantageous. In other fiber-reinforced fish skins, skin thickness has been shown to negatively relate with mechanical properties [37,45]. Notably, the correlation between skin thickness and collagen fiber angle was the only non-significant one. Although these morphological features sometimes seem to vary in unison, they do not appear to be related.

The relationships between collagen fiber angle and mechanical behaviors of the skin among batoids appear complex – likely a result of their dorsoventrally-compressed morphology. For instance, we found that the axial-undulators had skin with small relative fiber angles and their skin was the strongest and stiffest, whereas skin from the semi-oscillators and oscillators contained large collagen fiber angles and was less extensible, strong, stiff, and tough than the undulators. Adding complexity into morphological-mechanical relationships, denticle density positively correlated with mechanics (tensile strain, strength, stiffness, and toughness) whereas collagen fiber angle negatively correlated with all four behaviors (tensile strain, strength, stiffness, and toughness) and denticle density (Table 2). These relationships suggest that batoid skin becomes mechanically greater (stronger, stiffer, tougher) as collagen fiber angles become smaller (narrower) and as denticles are more densely arranged. The negative relationship between denticle density and collagen fiber angles has also been noted among sharks, and denticle density has been positively correlated with stiffness [36], and strength and toughness [37]. Although denticle density has previously been associated with greater mechanical properties, generally it is not positively linked to extensibility, as observed here. Though this relationship could be a spurious correlation among undulators who had the highest regional denticle density, these data may indicate that batoid denticles impact skin mechanics in a unique way compared to the denticles of sharks.

4.7. Density and diversity of dermal denticles

Due to the potential contribution of dermal denticles to mechanical properties of fish skin, we hypothesized that batoids with denticles (axial-undulators and undulators) would have greater skin strength and toughness than batoids with fewer or no visible denticles (semi-oscillators and oscillators). Among functional swimming groups, the axial-undulators and undulators had the toughest skin, and the axial-undulators had the strongest, stiffest skin. The density of dermal denticles was greatest among the undulators, whose skin was the most extensible. Additionally, the denticle density was higher among skin from the proximal disc region than the distal region (Fig. 2C). This finding makes sense given the need for protection closer to the vertebral axis and body center. We also observed dermal scales on the dorsal skin surface of each batoid species in this study, including those not previously identified in the literature (Fig. 10).

The potential impacts of dermal denticles on the mechanical properties of batoid skin may be a functional result of denticle morphology, rather than the density. The axial-undulators had the strongest and stiffest skin, and they have morphologically large, buckler denticles described as highly covering the bodies of fellow axial-undulating batoids, the guitar and thornback rays [29–31]. Dermal denticles may increase the mechanical rigidity of the skin through dense interlocking and overlapping, which can alter stiffness or strength [36,37,70]. Thus, the density of denticles among the axial-undulators is low because they have large denticles with minimal spacing. Conversely, the undulators had an arrangement of dense denticles emerging from central areas of the dermis and migrating outward radially. This results in a broad range of denticle density measurements among undulating batoids. The denticles are smaller prickles and thorns that disperse at a high density from a central pore or potentially pit organ and so may not overlap and interlock (Fig. 10). These smaller denticles (<20 μm) in the skin of undulatory species have not been well described, and classification and identification of these scales will require further research. Results of this study suggest that undulators have the most extensible skin among groups (Fig. 3). Extensible skin may therefore necessitate more denticles to create epidermal gaps (allowing for greater elongation), although the functional role of the denticles in modulating the mechanical behaviors of batoid skin warrants further investigation. Lastly, the composition of these denticle structures is not clear. If they are true denticles, the structures would consist of enameloid and dentine. However, if the structures also contain mineralized cartilage or vary compositionally across batoid groups, they could have specific mechanical consequences. Future studies that include computed tomography and histological methods to classify batoid scales would be beneficial in understanding the influence of these microscopic denticle structures on the skin mechanics of this diverse group of fishes.

5. Conclusions

We examined the mechanical behavior of batoid skin from six species representing four swimming modalities, quantifying the variation across body regions, pectoral discs, sexes, and stress axes. Batoid swimming styles included axial undulation (Atlantic guitarfish), and pectoral undulation (Atlantic stingray, bluntnose stingray, yellow stingray), oscillation (cownose ray), and semi-oscillation (smooth butterfly ray). Among dorsal and ventral skin samples, the mechanical properties of the skin reflected functional differences among swimming styles and between disc regions. Due to the limitations of cross-hair-based strain measurement, these findings should be considered qualitatively meaningful, emphasizing trends rather than absolute values. The undulators had the most extensible skin, the axial-undulators had the strongest and stiffest skin, and both groups had tougher skin than the oscillating groups. Composite samples behaved mechanically anisotropic: more extensible along the longitudinal body axis and stronger, stiffer, and tougher stressed along the hoop axis. These data improve our understanding of the mechanical function of batoid skin among swimming styles, relationships between skin morphology and mechanical properties, and provide inspiration for new biomimetic materials. Results of this study also provide evidence of sex differences in the mechanical properties of Atlantic stingray skin. While mechanical behaviors from six diverse species are presented and ranges among four swimming styles are established, we did not have representation for each taxonomic group of batoids (e.g., skates, sawfish), some of which possess dermal denticles. Future studies could focus on the mechanical properties of batoid skin from these groups for use among larger evolutionary and phylogenetic comparisons.

Funding

This work was supported in part by the National Science Foundation Career Award to M.E.P. (194713), the Society for Integrative and Comparative Biology Grant in Aid of Research to M.E.H., and the National Save the Sea Turtle Foundation scholarships to M.E.H.

CRediT authorship contribution statement

Madeleine E. Hagood: Writing – review & editing, Writing – original draft, Visualization, Validation, Software, Methodology, Investigation, Funding acquisition, Formal analysis, Data curation, Conceptualization. **Joseph R.S. Alexander:** Investigation. **Stephen Kajiura:** Writing – review & editing, Resources. **Marianne E. Porter:** Writing – review & editing, Supervision, Resources, Project administration, Funding acquisition, Conceptualization.

Declaration of competing interest

The authors declare that they have no known competing financial interests or personal relationships that could have appeared to influence the work reported in this paper.

Acknowledgements

The authors thank collaborators at NOAA Fisheries, Mote Marine Lab (Sarasota, FL; Jack Morris), Florida FWCC, and Florida Keys Aquarium Encounters for specimens. We thank members of the Florida Atlantic Biomechanics Laboratory for assistance with dissections and manuscript feedback, including Jamie Knaub, Aubrey Clark, Dr. Lauren Simonitis, and Dr. Darien Satterfield.

Supplementary materials

Supplementary material associated with this article can be found, in the online version, at doi:10.1016/j.actbio.2025.07.070.

References

[1] L.J. Compagno, Phyletic relationships of living sharks and rays, Am. Zool 17 (1977) 303–322.
[2] L.J. Compagno, Systematics and Body Form, Johns Hopkins University Press, Baltimore, Maryland, 1999.
[3] J.D. McEachran, N. Aschliman, Phylogeny of Batoidea, CRC Press, Boca Raton, Florida, 2004.
[4] W. Klausewitz, Der lokomotionsmodus der flugelrochen (myliobatoidei), Zool. Anz 173 (1964) 110–120.
[5] C.E. Heine, Mechanics of Flapping Fin Locomotion in the Cownose ray, Rhinoptera bonasus (Elasmobranchii: Myliobatidae), Duke University, North Carolina, 1992.
[6] C.M. Breder, The locomotion of fishes, J. Artic. (1926).
[7] P.W. Webb, The biology of fish swimming, Mech. physiol. anim. swim. (1994) 4562.
[8] L.J. Rosenberger, M.W. Westneat, Functional morphology of undulatory pectoral fin locomotion in the stingray taeniura lymma (Chondrichthyes: dasyatidae), J. Exp. Biol. 202 (1999) 3523–3539.
[9] L.J. Rosenberger, Pectoral fin locomotion in batoid fishes: undulation versus oscillation, J. Exp. Biol. 204 (2001) 379–394.
[10] A.P. Summers, M.M. Koob-Emunds, S.M. Kajiura, T.J. Koob, A novel fibrocartilaginous tendon from an elasmobranch fish (Rhinoptera bonasus), Cell Tissue Res 312 (2003) 221–227.
[11] J.T. Schaefer, A.P. Summers, Batoid wing skeletal structure: novel morphologies, mechanical implications, and phylogenetic patterns, J. Morphol 264 (2005) 298–313.
[12] R.M.N. Alexander, Functional Design in Fishes, Hutchinson, 1967.
[13] D.E. Sasko, M.N. Dean, P.J. Motta, R.E. Hueter, Prey capture behavior and kinematics of the Atlantic cownose ray, Rhinoptera bonasus Zool. (Jena) 109 (2006) 171–181.
[14] H.G. Rosenblum, J.H. Long Jr., M.E. Porter, Sink and swim: kinematic evidence for lifting-body mechanisms in negatively buoyant electric rays Narcine brasiliensis, J. Exp. Biol. 214 (2011) 2935–2948.
[15] E.L. Blevins, G.V. Lauder, Rajiform locomotion: three-dimensional kinematics of the pectoral fin surface during swimming in the freshwater stingray Potamotrygon orbignyi, J. Exp. Biol. 215 (2012) 3231–3241.
[16] L.J. Macesic, D. Mulvaney, E.L. Blevins, Synchronized swimming: coordination of pelvic and pectoral fins during augmented punting by the freshwater stingray Potamotrygon orbignyi, Zoology 116 (2013) 144–150.
[17] C.R.L. Amaral, F. Pereira, D.A. Silva, A. Amorim, E.F. De Carvalho, The mitogenomic phylogeny of the Elasmobranchii (Chondrichthyes), Mitochondrial DNA A 29 (2018) 867–878.
[18] J.E. Fontanella, F.E. Fish, E.I. Barchi, R. Campbell-Malone, R.H. Nichols, N. K. Dinenno, J.T. Beneski, Two- and three-dimensional geometries of batoids in relation to locomotor mode, J. Exp. Mar. Biol. Ecol 446 (2013) 273–281.
[19] C.A. Wilga, G.V. Lauder, Biomechanics of locomotion in sharks, rays, and chimeras, Biol. sharks their relat. 5 (2004) 139–164.
[20] J.W. Smith, The life history of the cownose ray, rhinoptera bonasus (Mitchill 1815), in lower Chesapeake Bay, with notes manag. species (1980).
[21] C.R. Robins, G.C. Ray, A Field Guide to Atlantic coast fishes: North America, Houghton Mifflin Harcourt, Massachusetts, 1986.
[22] A. Rajaram, N. Ramanathan, in: S. Saha (Ed.), The Tensile Properties of Ray Fish Skin, Biomedical Engineering I, Pergamon, 1982.
[23] P.J. Motta, Anatomy and functional morphology of dermal collagen fibers in sharks, Copeia (1977) 454–464.
[24] U. Seegers, W. Meyer, A comparative view of the fundamentals of the structure and function of fish skin, Kleintierpraxis 54 (2009) 73–87.
[25] S.A. Wainwright, F. Vosburgh, J.H. Hebrank, Shark skin: function in locomotion, Sci. (1979) 202 (1978) 747–749.
[26] K.T. Du Clos, A. Lang, S. Devey, P.J. Motta, M.L. Habegger, B.J. Gemmell, Passive bristling of mako shark scales in reversing flows, J. R. Soc. Interface 15 (2018).
[27] M.D. Naresh, V. Arumugam, R. Sanjeevi, Mechanical behaviour of shark skin, 22 (1997) 431–437.
[28] M.D. Naresh, D. Das, N. Ramanathan, A study on the histology of Ray fish skin, Leath Sci 32 (1985) 99–106.
[29] M. Stehman, L. Burkel, Rajidae, in: J.C. Hureau (Ed.), Fishes of the North-eastern Atlantic and the Mediterranean, Springer, Unesco: Paris, 1984.
[30] B. Serra-Pereira, I. Figueiredo, I. Farias, T. Moura, L. Gordo, Description of dermal denticles from the caudal region of Raja clavata and their use for the estimation of age and growth, ICES J. Mar. Sci. 65 (2008) 1701–1709.
[31] L.F. De Melo, B.G. Andrade, J.F. De Souza, M.G. Silva, H. Stapai, E.Q. Lopes, R.E. G. Rici, Morphological description of dermic denticles of guitar ray (Pseudobatos horkelli), J Vet Med Anim Sci 4 (2022) 1097.
[32] N.E. Kemp, S.K. Westrin, Ultrastructure of calcified cartilage in the endoskeletal tesserae of sharks, J. Morphol 160 (1979) 75–101.
[33] R. Gravendeel, W. Van Neer, D. Brinkhuizen, An identification key for dermal denticles of Rajidae from the North Sea, Int. J. Osteoarchaeol 12 (2002) 420–441.
[34] J. Jestine, R.E. Johnston, C.P. Pearce, B. Tordoff, E. Sackett, R. Board, N. Thomas, K. Joshy, Connected microscopy to characterise the dermal denticle of Raja clavata, the Thornback ray, Microsc. Microanal. 28 (2022) 1338–1340.
[35] M. Carvalho, N. Lovejoy, Morphology and phylogenetic relationships of a remarkable new genus and two new species of neotropical freshwater stingrays from the Amazon basin (Chondrichthyes: potamotrygonidae), Zootaxa 2776 (2011) 13–48.
[36] S.B. Creager, M.E. Porter, Stiff and tough: a comparative study on the tensile properties of shark skin, Zoology 126 (2018) 154–163.
[37] M.E. Hagood, J.R.S. Alexander, M.E. Porter, Relationships in shark skin: mechanical and morphological properties vary between sexes and among species, Integr. Comp. Biol (2023).
[38] C.M. Breder, D.E. Rosen, Modes of reproduction in fishes, 1966.
[39] A. Dugger, Mating stingrays, Sea Front. 33 (1987) 352–354.
[40] S.M. Kajiura, A.P. Sebastian, T.C. Tricas, Dermal bite wounds as indicators of reproductive seasonality and behaviour in the Atlantic Stingray, Dasyatis sabina, Env. Biol. Fishes 58 (2000) 23–31.
[41] T. Taniuchi, Shimizu, Dental sexual dimorphism and food habits in the stingray Dasyatis akajei from Tokyo Bay, Japan, J. Jpn. Soc. Fish. Sci. 59 (1993) 53–60.
[42] S. Kajiura, T. Tricas, Seasonal dynamics of dental sexual dimorphism in the Atlantic stingray Dasyatis sabina, J. Exp. Biol 199 (1996) 2297–2306.
[43] S.E. Nordell, Observations of the mating behavior and dentition of the round stingray, Urolophus helleri, Env. Biol. Fishes 39 (1994) 219–229.
[44] M.S. Micozzi, Experimental study of postmortem change under field conditions: effects of freezing, thawing, and mechanical injury, J. Forensic Sci 31 (1986) 953–961.
[45] E.B.L. Kennedy, R.P. Patel, C.P. Perez, B.L. Clubb, T.A. Uyeno, A.J. Clark, Comparative biomechanics of hagfish skins: diversity in material, morphology, and movement, Zoology 145 (2021) 125888.
[46] S. Ranamukhaarachchi, S. Lehnert, S. Ranamukhaarachchi, L. Sprenger, T. Schneider, I. Mansoor, K. Rai, U. Häfeli, B. Stoeber, A micromechanical comparison of human and porcine skin before and after preservation by freezing for medical device development, Sci. Rep 6 (2016) 32074.
[47] C. Crawford, Comparison of Mechanical Properties of Skin from Pacific hagfish, Eptatretus stoutii, and Penpoint gunnel, Apodichthys flavidus, Friday Harbor Laboratories, Washington, 2012.

[48] C.S. Shea-Vantine, K.A. Galloway, D.N. Ingle, M.E. Porter, S.M. Kajiura, Caudal spine morphology and puncture performance of two coastal stingrays, Integr. Comp. Biol 61 (2021) 749–758.
[49] K.A. Galloway, M.E. Porter, Mechanical properties of the venomous spines of pterois volitansand morphology among lionfish species, J. Exp. Biol 222 (2019) jeb197905.
[50] G.M. Cavanaugh, Formulae and Methods of the Marine Biological Chemical Room, Marine Biological Laboratory, Woods Hole, Massachusetts, 1975.
[51] H. Yamada, F.G. Evans, Strength of biological materials, 1970.
[52] Y. Lanir, Y. Fung, Two-dimensional mechanical properties of rabbit skin—II, experimental results, J. Biomech 7 (1974) 171–182.
[53] K. Yamaguchi, J. Lavety, R.M. Love, The connective tissues of fish VIII, comparative studies on hake, cod and catfish collagens, Int. J. Food Sci. Technol 11 (1976) 389–399.
[54] M. Lighthill, Hydromechanics of aquatic animal propulsion, Annu Rev. Fluid. Mech 1 (1969) 413–446.
[55] W. Webb, Hydrodynamics and Energetic of Fish Propulsion (bulletin 190), 1975. Ottawa, Ontario.
[56] P.W. Webb, Form and function in fish swimming, Sci. Am (1984) 72–82.
[57] L.K. Jordan, Comparative morphology of stingray lateral line canal and electrosensory systems, J. Morphol 269 (2008) 1325–1339.
[58] M.R. Hebrank, J.H. Hebrank, The mechanics of fish skin: lack of an" external tendon" role in two teleosts, Biol. Bull 171 (1986) 236–247.
[59] R.M. Kaplan, D.A. Chambers, R.E. Glasgow, Big data and large sample size: a cautionary note on the potential for bias, Clin. Transl. Sci 7 (2014) 342–346.
[60] F.E. Fish, H. Haj-Hariri, A.J. Smits, H. Bart-Smith, T. Iwasaki, Y. Bar-Cohen, Biomimetic swimmer inspired by the manta ray, Biomim.: nat.-based innov. (2012) 495–523.
[61] A.J. Smits, Undulatory and oscillatory swimming, J. Fluid. Mech (2019) 874.
[62] E.L. Brainerd, Pufferfish inflation: functional morphology of postcranial structures in Diodon holocanthus (Tetraodontiformes), J. Morphol 220 (1994) 243–261.
[63] R.E. Shadwick, H.S. Rapoport, J.M. Fenger, Structure and function of tuna tail tendons, Comp. Biochem. Physiol. A: Mol. Integr. Physiol. 133 (2002) 1109–1125.
[64] A.J. Clark, C.H. Crawford, B.D. King, A.M. Demas, T.A. Uyeno, Material properties of hagfish skin, with insights into knotting behaviors, Biol. Bull 230 (2016) 243–256.
[65] L.J. Macesic, A.P. Summers, Flexural stiffness and composition of the batoid propterygium as predictors of punting ability, J. Exp. Biol. 215 (2012) 2003–2012.
[66] M.K. Gabler-Smith, D.J. Coughlin, F.E. Fish, Morphological and histochemical characterization of the pectoral fin muscle of batoids, J. Morphol 284 (2023) e21548.
[67] W.F. Gilly, E. Aladjem, Physiological properties of three muscle fibre types controlling dorsal fin movements in a flatfish, Citharichthys sordidus, J. Muscle Res. Cell Motil. 8 (1987) 407–417.
[68] F.E. Fish, C.M. Schreiber, K.W. Moored, G. Liu, H. Dong, H. Bart-Smith, Hydrodynamic performance of aquatic flapping: efficiency of underwater flight in the Manta, Aerospace 3 (2016) 20.
[69] S.G. Seamone, D.A. Syme, The ocellate river stingray (Potamotrygon motoro) exploits vortices of sediment to bury into the substrate, J. Fish. Biol 99 (2021) 1729–1734.
[70] M.A. Kolmann, D.R. Huber, M.N. Dean, R.D. Grubbs, Myological variability in a decoupled skeletal system: batoid cranial anatomy, J. Morphol 275 (2014) 862–881.